



LUND UNIVERSITY

Optical Diagnostics of Gasoline Compression Ignition

HCCI-PPC-Diffusion Combustion

Lundgren, Marcus

2017

Document Version:

Publisher's PDF, also known as Version of record

[Link to publication](#)

Citation for published version (APA):

Lundgren, M. (2017). *Optical Diagnostics of Gasoline Compression Ignition: HCCI-PPC-Diffusion Combustion*. [Doctoral Thesis (compilation), Combustion Engines]. Department of Energy Sciences, Lund University.

Total number of authors:

1

General rights

Unless other specific re-use rights are stated the following general rights apply:

Copyright and moral rights for the publications made accessible in the public portal are retained by the authors and/or other copyright owners and it is a condition of accessing publications that users recognise and abide by the legal requirements associated with these rights.

- Users may download and print one copy of any publication from the public portal for the purpose of private study or research.
- You may not further distribute the material or use it for any profit-making activity or commercial gain
- You may freely distribute the URL identifying the publication in the public portal

Read more about Creative commons licenses: <https://creativecommons.org/licenses/>

Take down policy

If you believe that this document breaches copyright please contact us providing details, and we will remove access to the work immediately and investigate your claim.

LUND UNIVERSITY

PO Box 117
221 00 Lund
+46 46-222 00 00

Optical Diagnostics of Gasoline Compression Ignition

Optical Diagnostics of Gasoline Compression Ignition HCCI-PPC-Diffusion Combustion

by Marcus Lundgren



LUND
UNIVERSITY

DOCTORAL DISSERTATION

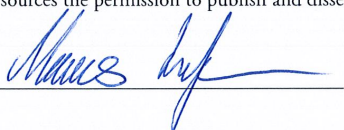
To be presented, with the permission of the Faculty of Engineering of Lund University,
for public criticism in the M:B lecture hall at the M-building, LTH on Sunday, the 2nd of
June 2017, at 10:15.

Faculty opponent: Professor Jesús V. Benajes, CMT-Motores Térmicos, Spain

Organization LUND UNIVERSITY Department of Energy Sciences Box 188 SE-221 00 LUND Sweden		Document name DOCTORAL DISSERTATION	
		Date of disputation 2017-06-02	
Author(s) Marcus Lundgren		Sponsoring organization Volvo AB Swedish Energy Agency	
Title and subtitle Optical Diagnostics of Gasoline Compression Ignition: HCCI-PPC-Diffusion Combustion			
Abstract <p>Diesel engines have become widely used for transportation in the commercial sector. These engines are attractive as they have low fuel consumption, but are also associated with high emissions of air pollutants, such as NO_x and soot. These emissions are directly toxic to human beings and some contribute strongly to the global warming.</p> <p>To face these issues, researchers have shifted focus to advanced combustion concepts, such as homogeneous charge compression ignition (HCCI) and partially premixed combustion (PPC). These concepts are two of many approaches known under the collective name of low temperature combustion (LTC). In conventional diesel combustion (CDC), fuel autoignites almost immediately and burns continuously as it is introduced in the combustion chamber. By contrast, LTC uses large amounts of exhaust gas recirculation (EGR), which extends the ignition delay and facilitates premixing of fuel and air before autoignition, thereby avoiding soot and NO_x formation while achieving high efficiency. These concepts are limited to low load operation. To extend the load range, gasoline has proved attractive due to its high resistance to autoignition. In contrast to diesel, this feature allows LTC to be used at increased loads. Despite the benefits, LTC concepts are challenged by high UHC and CO emissions, especially at low loads. At high loads, high pressure rise rates due to long ignition delays become challenging. For this reason, gasoline LTC cannot be achieved over the full load range and consequently CDC-like combustion needs to be used at high load. Nevertheless, gasoline has proven beneficial at high loads as well, producing less soot than diesel combustion.</p> <p>Gasoline compression ignition exhibits both opportunities and challenges as an approach to achieve cleaner engines. This work addresses the underlying factors, using a newly built optical engine to visualise the combustion processes. The study covers the whole load range, linking the concepts of low to medium load LTC to high load, CDC-like gasoline combustion. The first part of the results presents a transition from HCCI to PPC, coupling the combustion characteristics to the level of premixing and the combustion chamber bulk temperature. The second part describes a likely cause of UHC and suggests a potential method to reduce the, using multiple injections. In this study, laser diagnostics are used to trace the fuel distribution. Second to last, an intermediate load step between PPC and high load is described, addressing the difficulties of high pressure rise rates by utilizing double injection strategies. The last part presents high load gasoline operation and the factors behind soot reduction in comparison to diesel combustion. These results provides a wide but collective baseline of the fundamentally different combustion modes in gasoline compression ignition, linked over the whole load range.</p>			
Key words Optical engine, LTC, HCCI, PPC, Gasoline, High load			
Classification system and/or index terms (if any)			
Supplementary bibliographical information		Language English	
ISSN and key title 0282-1990		ISBN 978-91-7753-311-5 (print) 978-91-7753-312-2 (pdf)	
Recipient's notes		Number of pages 195	Price
		Security classification	

I, the undersigned, being the copyright owner of the abstract of the above-mentioned dissertation, hereby grant to all reference sources the permission to publish and disseminate the abstract of the above-mentioned dissertation.

Signature



Date

2017-05-04

Optical Diagnostics of Gasoline Compression Ignition

HCCI-PPC-Diffusion Combustion

by Marcus Lundgren



LUND
UNIVERSITY

A doctoral thesis at a university in Sweden takes either the form of a single, cohesive research study (monograph) or a summary of research papers (compilation thesis), which the doctoral student has written alone or together with one or several other author(s).

In the latter case the thesis consists of two parts. An introductory text puts the research work into context and summarizes the main points of the papers. Then, the research publications themselves are reproduced, together with a description of the individual contributions of the authors. The research papers may either have been already published or are manuscripts at various stages (in press, submitted, or in draft).

Cover illustration front: The natural luminosity of homogeneous charge compression ignition (HCCI), partially premixed combustion (PPC), and diffusion combustion.

© Marcus Lundgren 2017

Division of Combustion Engines
Department of Energy Sciences
Faculty of Engineering
Box 188
SE-221 00 LUND
Sweden

ISBN: 978-91-7753-311-5 (print)
ISBN: 978-91-7753-312-2 (pdf)
ISRN: LUTMDN/TMHP-17/1130-SE
ISSN: <0282-1990>

Printed in Sweden by Tryckeriet i E-huset, Lund University, Lund 2017

Till min bror och mina föräldrar.

Abstract

Access to clean and affordable energy is one of the cornerstones of the world's society. Since the introduction of the internal combustion engine, diesel engines have become widely used for transportation in the commercial sector. These engines are attractive as they have low fuel consumption, but are also associated with high emissions of air pollutants, such as NO_x and soot. These emissions are directly toxic to human beings and some contribute strongly to the global warming.

To face these issues, researchers have shifted focus to advanced combustion concepts, such as homogeneous charge compression ignition (HCCI) and partially premixed combustion (PPC). These concepts are two of many approaches known under the collective name of low temperature combustion (LTC). In conventional diesel combustion (CDC), fuel autoignites almost immediately and burns continuously as it is introduced in the combustion chamber. By contrast, LTC uses large amounts of exhaust gas recirculation (EGR), which extends the ignition delay and facilitates premixing of fuel and air before autoignition, thereby avoiding soot and NO_x formation while achieving high efficiency. These concepts are limited to low load operation. To extend the load range, gasoline has proved attractive due to its high resistance to autoignition. In contrast to diesel, this feature allows LTC to be used at increased loads. Despite the benefits, LTC concepts are challenged by high UHC and CO emissions, especially at low loads. At high loads, high pressure rise rates due to long ignition delays become challenging. For this reason, gasoline LTC cannot be achieved over the full load range and consequently CDC-like combustion needs to be used at high load. Nevertheless, gasoline has proven beneficial at high loads as well, producing less soot than diesel combustion.

Gasoline compression ignition exhibits both opportunities and challenges as an approach to achieve cleaner engines. This work addresses the underlying factors, using a newly built optical engine to visualise the combustion processes. The study covers the whole load range, linking the concepts of low to medium load LTC to high load, CDC-like gasoline combustion. The first part of the results presents a transition from HCCI to PPC, coupling the combustion characteristics to the level of premixing and the combustion chamber bulk temperature. The second part describes a likely cause of UHC and suggests a potential method to reduce the, using multiple injections. In this study, laser diagnostics are used to trace the fuel distribution. Second to last, an intermediate load step between PPC and high load is described, addressing the difficulties of high pressure rise rates by utilizing double injection strategies. The last part presents high load gasoline operation and the factors behind soot reduction in comparison to diesel combustion. These results provides a wide but collective baseline of the fundamentally different combustion modes in gasoline compression ignition, linked over the whole load range.

Populärvetenskaplig sammanfattning på svenska

I dagens samhälle är förbränningsmotorn den enväldigt största energiomvandlaren inom transportsektorn. I stort sett påverkas hela världens befolkning av den, exempelvis som patient i en ambulans, vid inköp av grönsaker i den lokala matbutiken, eller vid nöjesturen med motorcykeln på de slingriga vägarna kring Österlen. Som konsekvens av dess funktion, är att förbränningsmotorn har en stor påverkan på både hälsa och miljö, både lokalt i form av smog samt den globalt i form av växthuseffekten. Dessa problem ökar kontinuerligt med en ökad befolkning och högre levnadsstandard. För att stävja utvecklingen införs kontinuerligt allt strängare lagstiftning på utsläpp, vilket i sin tur uppmuntrar till ny forskning. Där inkluderat hybrida lösningar, helelektriska fordon, nya förbränningskoncept och fortsatt utveckling av befintliga koncept. Med det sagt är det en kraftigt konkurrensutsatt marknad där likaväl en ekonomisk vinst är lika nödvändig som att miljöpåverkan måste reduceras, vilket bidrar till en allt annat än trivial ekvation.

I dagsläget dominerar fordonen bensin och dieselmotorer våra vägar, båda typer med sina egna för och nackdelar. Bensinmotorer har sen införandet av trevägskatalysatorn, mycket låga utsläpp. Däremot har de lägre verkningsgrad än dieselmotorer, vilket i sin tur ökar utsläppen av koldioxid samt oförbrända kolväten. Dieselmotorer har hög verkningsgrad, men desvärre även höga utsläpp av kväveoxider och sot, vilket leder till dyra efterbehandlingssystem i form av SCR-katalysator och partikelfilter. Dessa typer av efterbehandling har en negativ effekt på förbränningen då det påverkar avgasernas flöde ut ur motorn.

Bensin och dieselmotorer är i grunden båda fyrtaktsmotorer av samma princip, däremot är deras förbränningstyper signifikant olika, vilka är källan till dess för och nackdelar. Bensinmotorer, förlitar sig på en gnistandändning av en homogen blandning av luft och bränsle, följt av en förbränning genom flamutbredning. Detta bidrar till en långsam förbränning som i sin tur påverkar verkningsgraden negativt. En homogen blandning behöver likaså lång tid att förblandas, där en konsekvens blir att bränsle blir fångat i skrymslen i förbränningskammaren, därav högre oförbrända kolväten. Dieselmotorer, fungerar genom att enbart luft komprimeras tills dieselbränsle sprutas in och självantänder. Förbränningen sker sedan kontinuerligt i en diffusionflamma, likt en eldsprutare på festival. Eftersom bränslet i detta fall förbränns kontinuerligt under kort förblandning fås en hög förbränningsverkningsgrad, över 99%. Dessa förhållanden får dock konsekvenser som; att bränslet pga. av dess lättantändligt brinner under rika förhållanden och producerar mycket sot, likaså blir denna typ av förbränning mycket varm vilket gynnar produktionen av kväveoxider.

Forskning om nya koncept har visat att det möjligt att kombinera fördelarna med respektive bensin och dieselmotorer. Genom att tillämpa kompressionsantänd lågtemperatursförbränning, som går under samlingsnamnet (Low temperature combustion - LTC), så har man gjort det möjligt att undvika varma och rika förhållanden. Genom att återcirkulera avgaser,

tillåts lång förblandning av luft och bränsle, utspädningen minskar således sotbildning och ger lägre förbränningstemperatur. Förbränningen blir också snabb, som i sin tur bidrar till en högre verkningsgrad.

Mängden varianter av LTC är många, men de som behandlas i denna avhandling är Homogenous Charge Compression Ignition (HCCI) och Partially Premixed Combustion (PPC), vilka kortfattat främst skiljer sig i strategi för luft och bränsle omblandning innan förbränningen börjar. Precis som andra koncept lider även dessa av nackdelar. Dels med svårigheter i kontroll av förbränningen samt möjligheter att nå högre last utan att skada motorn. Därför används olika förbränningskoncept vid olika last, t.ex. LTC vid låg last för att sedan återgå till diffusionsförbränning vid högre last. Genom att använda högoktaniga bränslen, likt bensin, har man visat ytterligare förbättringar i verkningsgrad samt har det visat sig fördelaktigt då mängden sot reducerats vid hög last.

För att få en förståelse bakom mekanismerna till vad som bidrar till de positiva och negativa aspekterna från förbränningskoncept kan man använda optiska mätmetoder. Kort beskrivet, filma förbränningsförloppet genom fönster till förbränningsrummet.

Denna avhandling använder sig av just optiska mätmetoder för att skapa en förståelse kring förbränning av högoktaniga bränslen, lika bensin, under kompressionsantändning. För att möjliggöra dessa mätningar har en ny experimentmotor byggts med optisk access som tål de höga påfrästningar och tryck som höglast har. Hela kedjan från HCCI, via PPC, till höglast med diffusionsförbränning behandlas.

Man har genom dessa mätningar visat hur förbränningen påverkas av hur väl förblandat luft och bränsle är samt dess temperaturkänsligheten vid HCCI, och hur känsligheten minskar vid en övergång till PPC. Med andra ord från en homogen luft och bränsleblandning, via kaotiska-, till stabila förhållanden med flertalet jämt fördelade förbränningszoner. Slutligen har höglast studerats i en jämförelse mellan diesel och bensin, där faktorer som påverkar sotbildning analyserats.

Övergripande, så har man för första gången visat helt olika förbränningsprocesser länkade över ett lastspectra. Denna kunskap kan sedan användas i utvecklingen av nya motorer, validera simuleringsmodeller, och skapa grundläggande förståelse för kompressionsantändning av bensin i en motor.

List of publications

- I **Gasoline PPC: A Parametric Study of Late Cycle Mixing Conditions using a Predictive Two-zone SRM Modeling Tool**
Marcus Lundgren¹, Martin Tunér¹, Bengt Johansson¹, Simon Bjerkborn², Karin Frojd², Arne Andersson³, Bincheng Jiang³, Fabian Mauss⁴
¹*Division of Combustion Engines, Lund University, Sweden*
²*LOGE AB*
³*Volvo AB*
⁴*BTU Cottbus*
SAE Technical Paper 2013-01-2621
- II **Optical Study on Combustion Transition from HCCI to PPC with Gasoline Compression Ignition in a HD Engine**
Marcus Lundgren¹, Öivind Andersson¹, Bengt Johansson¹, Joakim Rosell², Mattias Richter², Marcus Aldén², Arne Andersson³
¹*Division of Combustion Engines, Lund University, Sweden*
²*Division of Combustion Physics, Lund University, Sweden*
³*Volvo AB*
SAE Technical Paper 2016-01-0768
- III **Effects of post-injections strategies on UHC and CO at gasoline PPC conditions in a Heavy-duty optical engine**
Marcus Lundgren¹, Öivind Andersson¹, Martin Tunér¹, Zhenkan Wang², Alexios Matamis², Mattias Richter², Marcus Aldén², Arne Andersson³
¹*Division of Combustion Engines, Lund University, Sweden*
²*Division of Combustion Physics, Lund University, Sweden*
³*Volvo AB*
SAE Technical Paper 2017-01-0753
- IV **Lift-off Lengths of Gasoline and Diesel at High Load Operation in a Optical Heavy-Duty Engine**
Marcus Lundgren¹, Öivind Andersson¹, Pablo Garcia¹, Zhenkan Wang², Alexios Matamis², Mattias Richter², Marcus Aldén², Arne Andersson³
¹*Division of Combustion Engines, Lund University, Sweden*
²*Division of Combustion Physics, Lund University, Sweden*
³*Volvo AB*
To be submitted to Fuels Journal

v **Sensitivity Analysis Study on Ethanol Partially Premixed Combustion**

Mehrzhad Kaiadi¹, Bengt Johansson¹, Marcus Lundgren¹, John Gaynor²

¹*Division of Combustion Engines, Lund University, Sweden*

²*Scania CV AB*

SAE International Journal of Engines, 2013-01-0269

vi **Experimental Investigation on different Injection Strategies for Ethanol Partially Premixed Combustion**

Mehrzhad Kaiadi¹, Bengt Johansson¹, Marcus Lundgren¹, John Gaynor²

¹*Division of Combustion Engines, Lund University, Sweden*

²*Scania CV AB*

SAE Technical Paper 2013-01-0281

All papers are reproduced with permission of their respective publishers.

Acknowledgements

I would foremost like to thank my main supervisors *Prof. Öivind Andersson* and *Prof. Bengt Johansson*. *Bengt* had the pleasure (I presume) of hiring me. He gave me the trust in building and designing my lab. I can today, with confidence, say that the build plan reached a semi-solid progress of 100%. Three quarters through my PhD work, *Öivind* had the pleasure (I presume) to continue the supervision. He truly supported me through the last year, involving experiments and thesis writing. I'm equally grateful to you both. I believe that the combination of your knowledge and research mindsets made me (perhaps a bit pompously expressed) "*Ad utrumque*".

I would also like to thank my co-supervisor *Martin Tunér*. I really appreciate the support during my first year. Equally appreciated is the non-research engine related discussions. Another thanks goes to *Arne Andersson* at Volvo AB.

Thanks to *The technicians*. I've had the sincere pleasure to spend many hours in the lab and workshop with you. I appreciate the help I received and the discussions we had, and still are having concerning the technical conundrums related to research engines. Great fun!

Zhenkan, Panagiota, Alexios and Joakim from Combustion Physics. I really enjoyed the time we spent carrying out experiments, achieving great results and one or two perhaps not so great Zorbas.

I would like to acknowledge all my fellow colleagues and friends at the Division of Combustion Engines. I would especially like to raise a toast for *Pablo Garcia*, *Guillaume Lequien*, *Slavey Tanov*, *Tianhao Yang*. Gracias. Merci. Danke. Xièxie.

Last but not least my supportive parents, *Göran* and *Monika*, and my brother *Magnus*, thank you for your support and understanding. I plan to be free on my spare time from now on. Promise.

Nomenclature

aTDC	- After Top Dead Center
BDC	- Bottom Dead Center
CA ₅₀	- Crank Angle degree at 50% heat release completion
CAD	- Crank Angle Degree
CDC	- Conventional Diesel Combustion
CI	- Compression Ignition
CN	- Cetane number
CO	- Carbon monoxide
CO ₂	- Carbon dioxide
DI	- Direct Injected
EGR	- Exhaust Gas Recirculation
EOI	- End Of Injection
FSN	- Filtered Smoke Number
HCCI	- Homogeneous charge compression ignition
ID	- Ignition Delay
IMEP _g	- Gross Indicated Mean Effective Pressure
IVC	- Inlet Valve Closing
LIF	- Laser Induced Fluorescence
LoL	- Lift off Length
LTC	- Low Temperature Combustion
MK	- Modulated Kinetics
MK _I	- Environmental Class I Swedish diesel
NL	- Natural Luminosity
NO _x	- Nitrogen Oxides
PCI	- Premixed Compression Ignition
PLIF	- Planar Laser Induced Fluorescence
PM	- Particulate Matter
PPC	- Partially Premixed Combustion
PRF	- Primary Reference Fuel
PRF ₈₇	- PRF with 87% iso-octane and 13% <i>n</i> -heptane
RON	- Research octane number
SI	- Spark ignition
SOC	- Start Of Combustion
SOI	- Start Of Injection
TDC	- Top Dead Center
UHC / HC	- Unburned HydroCarbons

Contents

Abstract	i
Populärvetenskaplig sammanfattning på svenska	ii
List of publications	iv
Acknowledgements	vi
Nomenclature	vii
1 Introduction	1
1.1 Background	1
1.2 Objective and scope	3
2 Compression ignition combustion	5
2.1 Combustion in internal combustion engines	5
2.2 Conventional diesel combustion (CDC)	7
2.3 Low temperature combustion (LTC)	11
2.3.1 Homogeneous charge compression ignition (HCCI)	11
2.3.2 Modulated kinetics (MK)	12
2.3.3 Partially premixed combustion (PPC)	14
2.4 Use of high octane fuels in compression ignition	16
2.5 Research motivations	17
3 Experimental apparatus and diagnostics	19
3.1 Optical engines	19
3.1.1 History	20
3.1.2 Approaches in optical systems	21
3.2 Optical engine design and specifications	21
3.2.1 Limitations	24
3.2.2 Auxiliary systems	26
3.3 Diagnostics	26
3.3.1 High speed video	27
3.3.2 Laser diagnostics	27
3.3.3 Heat release analysis	29
4 Results and discussion	33
4.1 Kinetically controlled combustion	33

4.1.1	HCCI	33
4.1.1.1	Transition from HCCI to PPC	35
4.1.2	PPC	38
4.1.2.1	Post injections	40
4.1.3	Intermediate	42
4.1.3.1	o-D simulations	44
4.1.3.2	Pilot injections	47
4.2	Diffusion combustion	50
4.2.1	Gasoline versus diesel	51
4.2.1.1	Lift off length	52
5	Summary	57
5.1	Thesis contributions	58
6	Bibliography	61
7	Summary of papers	69
7.1	Paper I	69
7.2	Paper II	70
7.3	Paper III	70
7.4	Paper IV	71
7.5	Paper V	72
7.6	Paper VI	72

Chapter 1

Introduction

1.1 Background

The main energy converter in transportation is the combustion engine, and has been so during the last 100 years, and will likely be so for many years to come. The combustion engine is used in a vast number of applications, all from the smallest radio controlled leisure vehicles, ambulances, to cross Atlantic cargo ships. It is used in electricity production and auxiliary backup systems and delivers our vegetables to the local grocery store. The examples are many and the benefits and comfort for the society cannot be neglected. As all other inventions there are challenges, and no energy comes for free.

The history of the combustion engine is long. The reciprocating piston engine was widely recognised when Newcomen and Watt revolutionised the steam engine in the 1800th century [1]. The initial purpose of the steam engine was to pump water out from mines, which was clear improvement to the manual labour done by animals or humans. The applications expanded to propel machines in industry, trains and so forth. The steam engine was large, heavy and had low power, thus other solutions were needed. The breakthrough came after Nicholas Otto invented the spark ignited (SI) internal combustion engine (ICE) in 1876. Closely followed in 1892 by the introduction of the compression ignited (CI) diesel engine, named after its inventor Rudolf Diesel [1]. The new ICE was greatly reduced in size and weight, while the power increased. With its small size the engine could be mounted on vehicles for public transport. According to earlier standards, the combustion engine had "no" emissions, compared to horses that still were used for transport. As the animal emissions (faeces) disappeared, so did the diseases that came with it. This greatly improved the local environment in cities. These factors among others lead to that the four stroke engine came to be the main power source in transportation.

The emissions from the combustion engine was first recognised in the 1950's due to smog in California, USA, which greatly degraded the local environment. In the 1960's, the first legislation were set in California [2]. It took an additional 30 years before the legislations reached Europe, in 1992 [3]. The legislated emissions are carbon monoxide (CO), unburned hydro carbons (HC), nitrogen oxides (NO_x), particulate matter (PM)(soot) and particle number (PN), according to Euro VI [3]. The engine out emissions does also contain of (N_2), water (H_2O), and carbon dioxide (CO_2) which are not legislated. All these emissions affect both our global and local environment.

Global emissions, or greenhouse gases, are mainly related with CO_2 . This is a non-toxic and naturally occurring gas in our atmosphere, but through the excessive combustion of fossil fuels the concentration increases, consequently causing global warming. The phenomena occurs as sunlight passes trough our atmosphere and heats the earths surface. When reflected, the greenhouse gases absorbs the heat and the energy is scattered in the atmosphere, consequently heating Earth [4]. Other emissions that affect the global warming are both water and NO_x (among other), where the latter contains N_2O , which even more absorbent than CO_2 [5].

The local emissions are NO_x (NO and NO_2), PM, CO and UHC. All these emissions are directly toxic to humans and animals and can in extreme cases cause lung cancer or other health issues. Their effect mainly becomes a consequence in cities with heavy traffic. Since the industrial revolution the combustion of fossil fuels (among other human activities) have steadily increased and future forecasts predict an continuously increasing energy demand.

A growing population and improved standard of living, has the consequence of a continuously increase in energy demand. Today the energy conversion through combustion adds up to 91% [6], thereby the combustion engine has a big role to play. According to the 2016 Exxon world energy outlook, the global transportation demand will continue to increase to 2040, as seen in Figure 1.1.a [7]. Gasoline and diesel are predicted to be the main fuels, even though alternative fuels are continuously developed. The energy need from commercial transportation is solely dominated by the heavy-duty on-road vehicles, Figure 1.1.b.

Alternatives as electrification, fuel cells, natural gas, among other, has been recognized as a possible path in decreasing the oil dependency, [8]. Electrification has gained attraction as it shown promising forecasts as local emissions can be greatly reduced [9], especially in major cities where emissions form combustion engines are an increasing problem. However, challenges are met in terms of battery performance in terms of power density, lifetime cost and so forth, therefore mainly found in the light-duty car sector [10]. Attempts of electrifications of heavy-duty vehicles, and ongoing research demonstrated promising data of electrified roads with continuous charging of the truck [11]. Before these system are fully developed and commercially available, propulsion will continue to be dominated by the combustion engine.

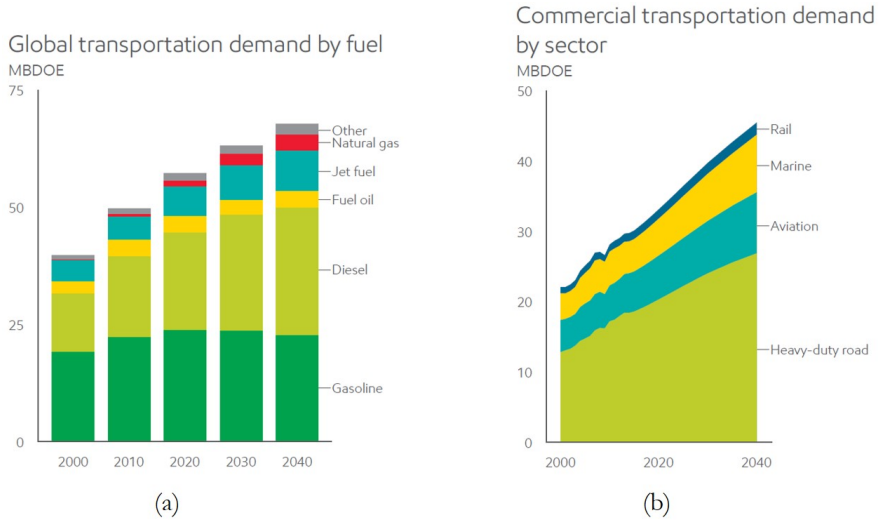


Figure 1.1: The global transportation energy demand by fuel, a), and sector, b). Million oil-equivalent barrels per day (MBOE) as a function of year. Reproduced from [7].

The engines, that were invented by Nicholaus Otto and Rudolf Diesel, are still the dominating in the transportation sector. The former, SI engine which is fueled by gasoline is mainly used in the light-duty sector in personal transportation. The latter CI diesel engine, is mainly used in the heavy-duty commercial sector. Diesel CI engines are especially attractive for the future due to their high fuel-efficiency compared to the SI engines, however, CI engines suffers with high emissions of NO_x and soot (local air pollutants). [2, 12].

Research during the last decade has shown that adavanced CI combustion processes with high octane fuels, such as gasoline, can be competitive in enabling high efficiency, while reducing NO_x and soot emissions to only fractions of the conventional diesel combustion (CDC) [13].

1.2 Objective and scope

The goal of this work is to answer questions and gain further knowledge about CI combustion fuelled with high octane-number fuels, with the objective to reduce local and global emissions. The focus here is on the coupling between different combustion modes and related engine loads, while describing and summarizing their characteristics, in terms of challenges and solutions.

The combustion modes that are investigated are, homogeneous charge compression ignition (HCCI) and partially premixed combustion (PPC), which both sort under the heading of

low temperature combustion (LTC). This is a collective name for the techniques achieving low engine out NO_x and soot through reduced combustion temperature. The next mode investigated is CDC-like combustion with high octane fuels. All these combustion types will be explained and developed in the following chapters.

The main part of the experiments are performed in a heavy-duty truck engine, modified for optical access. This is basically an engine with windows that unveil the combustion chamber. Much effort is spent on describing the design process and features of the optical engine, which is built to facilitate high load operation for this and future work.

The next chapter will provide background information to various combustion modes that leads up to the specific research motivation and results of this thesis.

Chapter 2

Compression ignition combustion

This chapter will introduce the different combustion modes used in this thesis. Initially this will be presented with an overview of existing combustion processes. The following sections will focus on CI, first reviewing CDC and then LTC. The penultimate section address the usage of high octane fuels in these combustion processes. The final section will present the research motivation of this thesis.

2.1 Combustion in internal combustion engines

To put the research motivations of this thesis into perspective, a review of existing combustion concepts needs to be addressed. To simplify this review a combustion triangle

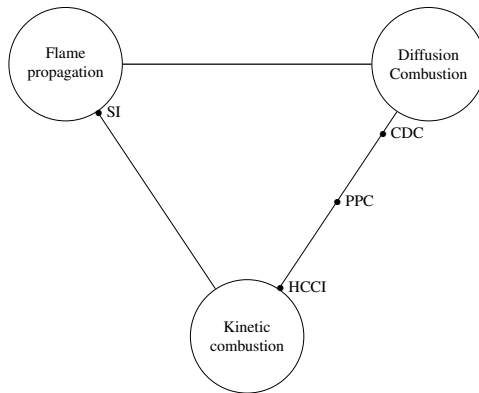


Figure 2.1: A schematic triangle where the different combustion types form the corners of a triangle. The combustion modes in this thesis are placed depending on their relation to each combustion type.

is formed, as depicted in Figure 2.1. This triangle categorizes the combustion processes, where flame propagation, diffusion and kinetic combustion forms the corners. These are per definition described below [14].

- Flame propagation is when a flame front or combustion propagates through a homogeneous combustible gas mixture, with the origin from an applied ignition source.
- Diffusion combustion occurs when fuel is continuously introduced as a separate entity during combustion. The fuel rapidly mixes with the ambient oxidizer, before the reaction occurs in the flame zone.
- Kinetic combustion occurs as a premixed fuel and air mixture spontaneously autoignite, and a rapid reaction, or even called explosion, with a series of propagating autoignitions takes place. This type of reaction is strongly controlled by the chemical composition, pressure and temperature .

The three corners in Figure 2.1 are connected which describes combination of combustion processes in between, such as a mix of kinetic and diffusion combustion. To be able to relate the combustion triangle to the combustion processes that occur in a internal combustion engine the principle of the four-stroke cycle needs to be understood.

This will be described with the cycle in traditional diesel engines, starting at the top dead center (TDC), where the piston is in its highest position. The first stroke contains the intake phase, where air (the oxidizer) is introduced to the cylinder via the open intake valves. This occurs during the downwards movement of the piston. When reaching the bottom dead center (BDC), the lowest position of the piston, the valves close and the piston changes direction. Next occurring is the compression stroke, where the introduced air is compressed, which consequently increasing the pressure and temperature. Close to TDC, diesel fuel is introduced to the combustion chamber and rapidly mixes with the air, before autoignition occurs due to the high temperature. The combustion continues in a diffusion flame as long as fuel is introduced into the combustion chamber. The energy which is released increases the pressure, and forces the piston down after passing TDC. This is called the power stroke. The final and fourth stroke is called the exhaust stroke and scavenges the burnt gases by opening the exhaust valves to the ambient condition. As the stroke reaches TDC, the process starts over.

Diffusion combustion or CDC will be described in detailed in the following section 2.2. Although, in the paragraph above, both autoignition and diffusion combustion are mentioned. These implies that the CDC contains a part of small kinetic combustion and a main diffusion combustion. This places CDC close, but not fully to the diffusion combustion corner in Figure 2.1.

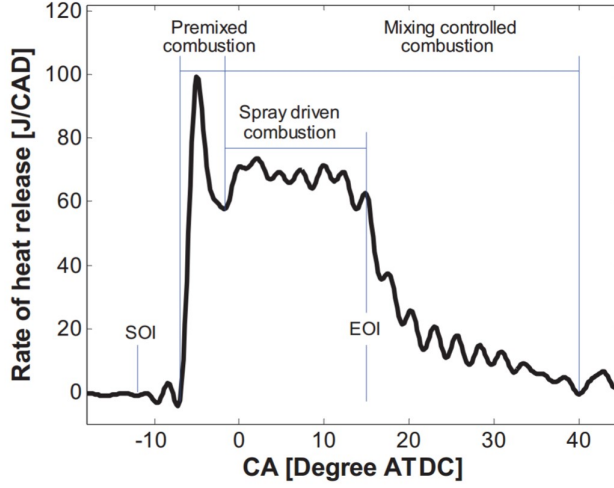


Figure 2.2: The rate of heat release of a conventional diesel combustion. Reproduced from [15]

The combustion engines in today's society are mainly spark ignited (SI) gasoline engines and diesel engines. In contrast to CDC, the fuel and air are premixed and introduced during the intake stroke and finally ignited by a spark close to TDC [2, 12]. Therefore, the combustion process is solely through flame propagation, and can be placed in the far end corner.

As introduced in section 1.2, this work is limited to the CI combustion, reaching from diffusion combustion to kinetic combustion in Figure 2.1. There are many concepts that can be placed in this area, but only the directly related to this work are explained here. The following subsections will start at top corner of diffusion combustion.

2.2 Conventional diesel combustion (CDC)

A typical CDC can be explained with a rate of heat release (RoHR), as seen in Figure 2.2. The RoHR, briefly described, is a representation of the combustion process, and will be presented in detail in section 3.3.3.

A typical diesel combustion is initiated with a start of injection (SOI), before TDC. The introduced liquid fuel vaporizes, and mixes with the ambient air. This is seen as negative values in the RoHR trace, since energy is taken from the combustion chamber to vaporize the fuel. This phase is called the ignition delay (ID). When fuel and air reaches a combustible mixture and temperature that allow ignition, autoignition occurs, and ends the ID. The start of combustion (SOC) is a premixed kinetic combustion, seen as a initially high

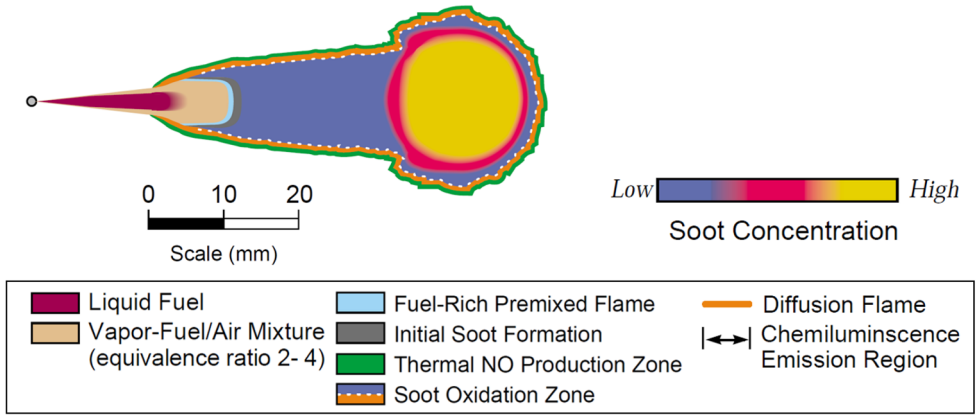


Figure 2.3: A model of a quasi-steady spray driven flame. Reproduced from 2.3

peak in the RoHR in Figure 2.2.

The next phase is referred to as the spray driven combustion. Here, a diffusion combustion establishes, and this continues as long as fuel is injected. After the end of injection (EOI), the RoHR decays as the remaining fuel is combusted. These two phases are under the mixing controlled combustion, meaning that the combustion rate is limited by the mixing of evaporated fuel and ambient air. Each phase of the RoHR curve is controlled by fuel injection parameters, such as timing (SOI), duration and injection pressure, but also the intake air composition and temperature and the fuel reactivity to autoignition.

The most widely used description of the CDC phenomenon was proposed by [16]. His work is based on optical laser diagnostics of diesel sprays inside a heavy duty engine. Figure 2.3 represent the quasi steady jet of the spray driven combustion phase. The figure illustrates a cut view through the centreline of the jet.

The model contains several zones which describe the process. The process is started from the left, where liquid fuel enters the combustion chamber through the injector nozzle, here marked as the grey dot. The liquid fuel, which is injected under high pressure, evaporates and mixes with the ambient air and surrounds the liquid core. Downstream from the mixture the fuel-rich premixed flame establishes, where the initial soot formation occurs. The soot particles are transported by the jet downstream where the soot becomes concentrated. The whole latter phases are surrounded by a diffusion flame, where most of the soot oxidation takes place and the thermal NO_x is formed. This model is highly dependent on engine operating conditions, which vary the length scales of the different zones.

CDC has a very short time for the fuel to evaporate and mix with air before combustion, as seen in Figure 2.3. Thereby, the combustion takes place under rich conditions. In later stages these fuel rich areas can be oxidized with the excessive air in the later phase of the

combustion, thus forming a global equivalence ratio Φ . Equation 2.1 describes this relation, defined by the ratio between the actual fuel and air ratio divided with the stoichiometric fuel and air ratio. Thereby a Φ -value of one means that there is precisely the amount of air needed for the fuel to be fully combusted. During CDC the fuel and air burns over a great variety of locally Φ s, thus a closer analysis of diffusion flame is needed.

$$\Phi = \frac{(F/A)_{actual}}{(F/A)_{stoichiometric}} \quad (2.1)$$

In 1996, Naber and Siebers developed a relation, of the local Φ in a non-combusting fuel jet, at distance x from the injector nozzle $\Phi(x)$ [17].

$$\Phi(x) = \frac{2 \cdot f_s}{\sqrt{1 + 16 \cdot \left(\frac{x}{x^+}\right)^2} - 1} \quad (2.2)$$

where f_s is the stoichiometric air-fuel ratio and x^+ is a characteristic length.

$$x^+ = \frac{d_f \sqrt{\frac{\rho_f}{\rho_a}}}{\tan\left(\frac{\alpha}{2}\right)} \quad (2.3)$$

where d_f is the injector nozzle orifice, ρ_f and ρ_a are the fuel density and air density respectively and α is the fuel spreading angle.

One of the central parts in diffusion combustion is the lift-off length (LoL), which is defined as the distance from the injector nozzle to the first most upstream flame of the burning jet. The LoL position H , was initially empirically established by [18], by measurement data retrieved in combustion vessels. Lequien *et al.* extended the calculation with data retrieved from optical engines [19].

$$H = B \cdot T_{bulk}^{-1.24} \cdot \rho_{bulk}^{-0.86} \cdot d^{0.56} \cdot U^{0.52} \cdot Z_{st}^{-1.06} \cdot R_s^{0.07} \cdot \theta^{0.5} \quad (2.4)$$

where B is a constant, T_{bulk} and ρ_{bulk} are the ambient gas temperature and density respectively, d is the nozzle orifice, U the fuel injection velocity at the nozzle and Z_{st} is stoichiometric mixture fraction. New factors to the expression are the swirl number, R_s and the inter jet angle θ .

The soot formation during the quasi steady jet phase is found to be affected by the LoL, as the large parts of the air entrainment to the jet occur upstream the position of the lifted

flame [20]. Therefore it is of interest to increase the LoL to allow more air entrainment upstream, which decrease the $\Phi(x)$ and consequently the soot formation.

Equation 2.4 suggest that the bulk temperature in the combustion chamber is one of the stronger factors to increase the LoL, which is in line with the previously derived equation from [18]. Other means of controlling the air entrainment include nozzle orifices and the bulk density.

NO_x and soot are the two most important emissions issues in a diesel engine and both are mainly due to the combustion process.

NO_x , which contains both NO and NO_2 , is mainly formed through oxidation of the atmospheric nitrogen. It can also be formed in fuel rich zones, when using fuels containing nitrogen. NO_x needs high temperature to be formed, which is the reason behind the large amount of NO_x that is produced in the diesel diffusion flame. In contrast to soot emissions, the formed NO_x is difficult to oxidise [2].

The engine out soot emissions are a combined process of formation and oxidation. The formation takes place in hot fuel rich conditions, followed by the oxidation which is dependent on high temperature and turbulence. This means that strategies to lower the soot formation can consequently decrease the soot oxidation, thus the engine out soot emissions might be unaffected.

Both the NO_x and soot formation zones can be described through a Φ -T map as seen in Figure 2.4. This map contains the calculated soot and NO_x formation zones for *n*-heptane, which is a surrogate fuel for diesel. The diagram was originally derived by [21], and complemented with arrow paths of the fuel elements through combustion [22]. The solid line is the adiabatic flame temperature for 21% O_2 content.

The open arrows line describes the CDC, passing through both of the emissions zones. Here, it is evident which Φ values and temperatures to avoid in order to decrease, or even evade, the emissions. During the recent decades new combustion strategies which allow low Φ and low temperature, by adding cooled exhaust gas recirculation (EGR) have been developed. Several studies found that a Φ value below two achieve close to smokeless combustion [23, 24, 25].

There are numerous strategies to avoid the soot and NO_x peninsulas in the Φ -T map. These strategies have a collective name, LTC, and will be discussed in the next section.

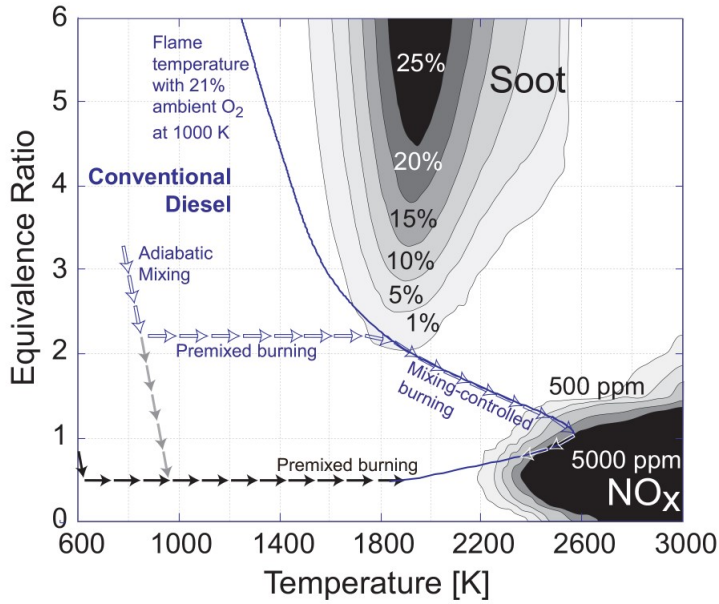


Figure 2.4: Φ -T map with, including CDC with open arrows, and two LTC variants with grey and black arrows. [22]

2.3 Low temperature combustion (LTC)

The fundamental concept of LTC is based on the principle of avoiding the soot and NO_x formation zones in Figure 2.4. This is accomplished by reducing both the combustion temperature and the Φ , while maintaining high efficiency through premixed or partially premixed kinetic combustion[26, 27].

This can be achieved with various strategies, but can be exemplified with a common denominator, the prolonged ignition delay by applying EGR. The EGR is introduced in the intake air and works as an inert gas, which slows down the kinetic reactions, thereby the ID increases, which enhances premixing and thus decreases the Φ . After the onset of combustion, EGR becomes a thermal buffer zone and thus decreases the combustion temperature below the NO_x formation zones. These process can be exemplified with the grey and black arrows in Figure 2.4, where the latter is typically associated with HCCI combustion.

2.3.1 Homogeneous charge compression ignition (HCCI)

HCCI combustion can very simplified be seen as a combination of traditional SI combustion and CDC. Like SI, the fuel is introduced in the intake port (or by direct injection during the intake stroke) and mixes into a homogeneous mixture during the intake and

compression stroke. In contrast to SI, the charge autoignites like CDC, but the fully premixed charge leads to a rapid combustion reaction [28, 29, 30].

The principle behind the HCCI concept was first mentioned in 1979 by Onishi *et al.*, but under the name Active thermo-atmosphere combustion (ATAC). The combustion process was realized in a two-stroke engine [31]. Based on the concept, the strategy was adapted to four-stroke engines by Thring [32].

HCCI is an attractive approach with which high thermal efficiency is achieved with ultra low emissions of NO_x and soot. The combustion principle is kinetically controlled, thus the reaction is very rapid and therefore, noise emissions through pressure rise rate (PPR) become high. To reduce it, increased EGR can retard the onset of combustion after TDC, and thereby reduce the maximum cylinder pressure [33].

The combustion process is highly related to the mixture composition at the point of SOC. Optical studies have shown that the combustion originates from a local area, which implies that the mixture is either not fully homogeneous or thermal stratification exists in the combustion chamber [34, 35]. After the first combustion kernel appears, a sequence of autoignition continues throughout the chamber, from hot regions to colder. Although, due to variations in the turbulence, the location of the onset of combustion is altered from cycle to cycle.

The major drawbacks with HCCI are limitations in achieving high load due to the high PPR and overall controllability, both effects related to the separation of injection and SOC. Other issues are high UHC caused by wall wetting, trapped fuel in crevice and cylinder wall quenching [30].

Various strategies can be applied to increase control robustness and load range of the combustion process, such as the concepts, premixed lean diesel combustion (PREDIC), reactivity controlled compression ignition (RCCI), and spark assisted compression ignition (SACI), to name a few [36, 37, 38]. With the same mission, partially premixed combustion (PPC) uses an injection during the last quarter of the compression stroke, close enough for the SOI to control the combustion phasing, while high EGR facilitates high efficiency and low NO_x and soot. The first published work with PPC-like combustion was the modulated kinetics (MK) by Nissan [39].

2.3.2 Modulated kinetics (MK)

In 1999, Kimura *et al.* presented the MK combustion, with the ambition to achieve low NO_x and smokeless combustion [39, 40]. In contrast to HCCI, the injection takes place close to after TDC. By utilizing large amount of cooled EGR, a sufficient ignition delay combined with high swirl allows the fuel and air to mix before auto-ignition. With this, the

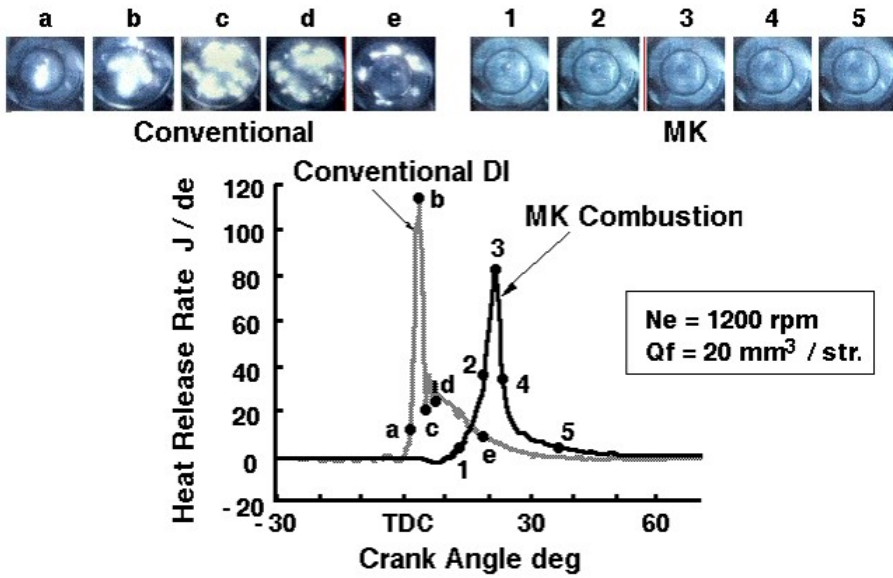


Figure 2.5: The difference between in heat release rate between conventional diesel, and MK combustion. Reproduced from [40].

pressure rise rate is effectively reduced since the combustion takes place late in the expansion cycle, while achieving low NO_x and soot emissions. Like HCCI, issues to reach high load showed to be a limitation.

To meet this issue, the compression ratio is reduced and the load range is thereby extended. The concept still suffers of short ignition delay, mainly due to two factors. Firstly, the ignition delay is decreased as the EGR gas temperature increased. Secondly, to provide the amount of energy required for higher loads, longer injection durations are needed, consequently decreasing the ignition delay.

A extended study of MK combustion was performed by Miles *et al.* [41]. This study describes how the first part of the combustion process is dominated by chemical kinetics, seen as rapid heat release between 1-3 in Figure 2.5, followed by a latter part with a mixing controlled process between 4-5, close to the CDC process between d-e. In contrast to the combustion images in Figure 2.5, optical diagnostics in [41] show soot rich pockets. These findings indicate a more partially premixed combustion than suggested by Kimura *et al.*. Due to the late combustion process, the MK combustion suffers from low combustion efficiency (high UHC and CO). The incomplete combustion is a consequence of the continuously decreasing temperature during the expansion phase, and late combustion phasing decreases the possible work to be applied on the piston.

Despite its limitations in efficiency and load, the MK combustion mode is the first where a relative short but still positive ignition delay (injection finished before ignition) is achieved. These features allow combustion phasing to be controlled while maintaining low NO_x and soot.

2.3.3 Partially premixed combustion (PPC)

In order to overcome the problems of both the HCCI and MK, a concept named PPC has been introduced [13]. In contrast to MK, the fuel is injected in the last quarter of the compression stroke. This fuel injection strategy in combination with high levels of EGR assure LTC, with high thermal efficiency while avoiding the soot and NO_x formation areas [42, 43, 44].

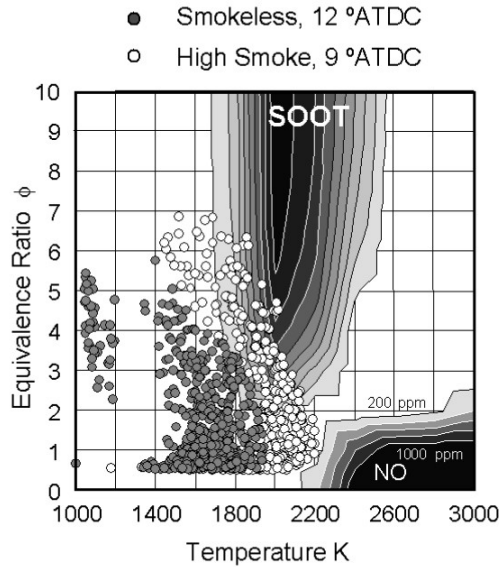


Figure 2.6: Φ -T map describing the difference between low soot and high soot combustion. Reproduced from [45]

In 2001, Akihama *et al.* performed numerical simulations to describe the mechanism for the low soot and NO_x emissions in their concept called smokeless rich diesel combustion [45]. Like PPC, the fuel injection occurs before TDC and high levels of EGR are used. Figure 2.6 describes the location of gas cells near maximum heat release for both smokeless and high smoke conditions. The only difference between the two, higher EGR for the smokeless condition. In Figure 2.6, it is evident that the decreased temperature is the main cause for the low soot production. The ignition delay lowers the equivalence ratio, although, gas cells are still seen in relatively high Φ levels even for the smokeless conditions. The NO_x

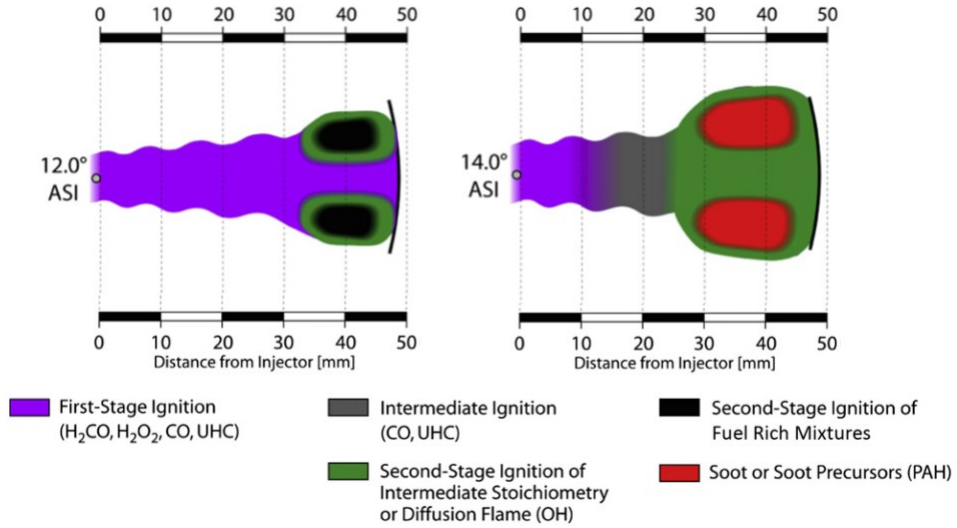


Figure 2.7: Conceptual model of diesel partially premixed LTC. Reproduced from [46]

formation zone is neither reached as the combustion temperature is reduced by the high EGR level.

Musculus *et al.* developed a conceptual model of diesel partially premixed LTC [46], as seen in Figure 2.7. Here, two stages of the combustion process at the maximum heat release shown, 12 CAD after start of injection (ASI) and 14 CAD ASI. Compared to the model presented by John Dec in Figure 2.3, PPC is fundamentally different. In contrast to CDC, the combustion occurs further downstream the jet, after the injection ends and when all the fuel is fully vaporized. The fuel forms locally fuel rich pockets, where the onset of combustion takes place, seen as the black areas in the model. As combustion progress in 14 CAD ASI, soot is formed and the pocket grows. After the maximum heat release is over the soot is oxidized and the clouds shrinks. At the end of combustion, the central regions close to the injector are still in the first stage ignition, marked with purple. This areas remains stagnant throughout the expansion and are therefore a source of engine out UHC.

These emissions are formed as a consequence of incomplete combustion, mainly caused by over-lean or over-rich conditions . There are two recognized areas where the combustion normally does not reach full combustion: the crevice volume and the central region in the combustion chamber [47].

UHC emissions from the central regions are partly a consequence of a rapid over-leaning immediately after EOI [48, 49]. This phenomenon is described to be a consequence of an entrainment wave [50]. After the end of injection, a region of enhanced air entrainment travels along the jet at approximately twice the velocity of the injected fuel. Modelling

indicates three times higher air entrainment rates into the jet compared to steady injection, accentuating the problems of over-lean mixtures close to the injector for LTC conditions.

Post injections have shown to be a viable approach to reduce these emissions and have been successful for diesel PPC [51, 52]. These studies analyse both the mass repartition and separation between the main and post injections. UHC are reduced both with small post injections, acting after SOC, and with large post injections acting close to the main injection and before SOC. Here, the latter shows the highest reduction. It is hypothesised that the close coupled post injections interact and push the main injection downstream the jet trajectory, thereby reaching further into the combustion chamber after impinging and mixing with the adjacent spray on the piston bowl wall.

Using diesel as fuel in PPC needs excessive amounts of EGR to ensure sufficient premixing to assure LTC, which leads to low load limitations. A long ignition delay is desired, for that reason fuels with high resistance to autoignition are suitable for PPC. The following section will discuss the benefits and drawbacks of high octane fuels.

2.4 Use of high octane fuels in compression ignition

Table 2.1: Fuel specifications. (Boiling point (BP))

Fuels	RON	CN	H/C	O/C	BP [°C]	Density [kg/m ³]	LHV [MJ/kg]
<i>iso-octane (PRF100)</i>	100	-	2.25	0	100	692	44.33
<i>n-heptane (PRF0)</i>	-	54.6	2.286	0	99.4	684	44.66
<i>PRF87</i>	87	-	-	-	≈100	689	-
<i>Gasoline</i>	87	-	1.92	0	20-160	726	43.5
<i>Diesel MKI</i>	-	54	1.87	0	160-380	813	43.15
<i>Ethanol</i>	107	-	3	0.5	78.37	789	26.9

Fuel properties are highly important parameters regarding LTC operation, and the possibilities of reaching higher loads. The usage of high octane fuels has received attention because of low smoke and NO_x emissions, while simultaneously reducing required levels of EGR, compared to diesel LTC [13, 53, 54].

Two important factors of the fuel properties are chemical reactivity (resistance to auto-ignition) and fuel volatility (ease of evaporation). The chemical reactivity is described as research octane number (RON) and cetane number (CN), where a high RON fuel has high resistance to auto-ignition and a high CN fuel has low resistance to auto-ignition. A high volatility fuel has a low boiling point, for example an alcohol which evaporate in room temperature. The benefits of using high RON fuels come mainly from these properties.

High RON fuels, such as gasoline facilitate longer ignition delay compared to high CN fuels, like diesel. The delay allows fuel and air to premix more, and thereby decrease soot

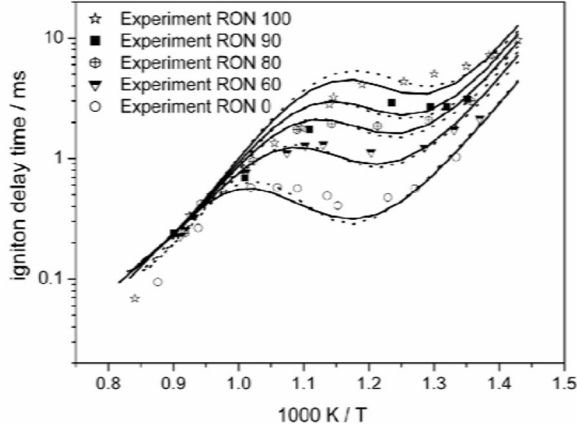


Figure 2.8: Ignition delay of different RON-fuels as a function of temperature. Reproduced from [58]

emissions. Gasoline is also a more volatile fuel than diesel. That means the liquid length decreases, which also promotes the fuel and air mixing prior to autoignition [55, 56].

Consequently, the long ignition delay leads to increasing CO and HC emissions, since overleaning can be an issue. The high RON does also lead to ignition difficulties at low loads and high EGR levels [57].

Table 2.1 contains the fuels that have been used in this work. No experiments have been performed with gasoline or diesel, however they are included for the sake of comparison.

This work uses primary reference fuels (PRF) to replicate the resistance to autoignition of gasoline and diesel. A PRF contains a blend of single-component fuels like iso-octane and *n*-heptane, which are defined as RON of 100 and 0 respectively [58, 59, 60]. As seen in Table 2.1, the properties in terms of density and BP (volatility) differ between the PRFs and the pump fuels, which consequently leads to variation in liquid length and injected fuel rate [61, 62]. Pump fuels, such as gasoline and diesel, are multi-component fuels and are thereby difficult to replicate for other studies and simulations. Figure 2.8 shows the ignition delay for PRF with RON between 0 and 100. This work mainly uses PRF87 (87% iso-octane and 13% *n*-heptane by volume).

2.5 Research motivations

Although several detailed studies have been made in the field of both LTC and diffusion combustion, much remains to be understood. The general motivation of this work is to relate LTC modes to diffusion combustion over the whole load range with high octane fuels, addressing the possibilities and challenges based on optical diagnostics. The motivations to

this work are listed below:

- To date, most studies of PPC in optical configuration is carried out in a swirling environment. For this reason, there is a lack of optical diagnostics in quiescent combustion systems.
- Due to the mechanical limitations of most optical engines, optical studies are mainly performed at lower load operation. For this reason, high load operation is less investigated. This requires the development of a new optical engine.
- High octane fuels have shown low emissions at high load, but optical investigations to explain the causes are yet to be performed.
- Since gasoline PPC suffers from UHC emissions, further investigations on the sources and means to decrease them are needed.
- There is a need to investigate the reasons for lower soot production at high load operation with high octane fuels.

The next chapter will describe the optical research engine and diagnostics methods used in the experiments presented in the results section.

Chapter 3

Experimental apparatus and diagnostics

To be able to answer the research question a new optical engine is designed and built, which can cope with high load operation without penalties of optical access. The base engine is a Volvo MD13, combines historical engine designs with new ideas in terms of strength, maintenance, access and durability. The main diagnostic methods used in the engine are high speed video (HSV) complemented with planar laser induced fluorescence (PLIF).

3.1 Optical engines

Various methods are used to study engine combustion, such as full engine testing, numerical simulations and optical diagnostics. All these approaches complement each other to create new knowledge and verify existing knowledge. Full engine research normally focuses on engine control, emissions, and efficiency, each with their own subcategories. During these types of research new questions emerge, which may be impossible to answer by full engine tests and require other types of diagnostic methods. One of the options is optical diagnostics, which mainly are used to investigate the detailed phenomena leading up to the question asked. This has become a common approach for engine research which is likely to be used for many years to come.

3.1.1 History

Already Nicolaus Otto, used optical diagnostics while developing his four-stroke cycle in 1872. He built a hand driven piston machine with a glass cylinder, where he let air be aspirated through cigarettes during the intake stroke. The idea was to visualize flow of the intake air during the engine cycles, while claiming that the separation between the cigarette smoke ("air and fuel mixture") and the in cylinder ambient gas would act as a dampening gas of the explosion. Although the claim of his display were wrong, this is the first known example of using an optical engine to study in-cylinder processes [63].

Sir Harry Ricardo continued with optical diagnostics in the late 1920's, using a side valve engine with a line of small windows across the cylinder head, allowing the measurement of flame speed. This idea was taken further in 1932 by Marvin and Best who added a matrix of small windows. Among other observations, they showed the linearity between flame speed and engine speed. Thus research question were becoming more complex, and the need of a continuous view of the combustion was needed, [63].

Withrow and Boyd developed an approach using a rotating quartz slit in the cylinder head, imaging the combustion on a synced camera film [64]. This allowed more detailed studies of the flame propagation and they could see how the instantaneous phenomena of knock rapidly occurred in front of the flame front in the unburned air and fuel mixture. A sketch of the design can be seen in Figure 3.1 (a). Eventually, full quartz windows were used both as cylinder head and as side view access, which in turn lead to fully optical liners.

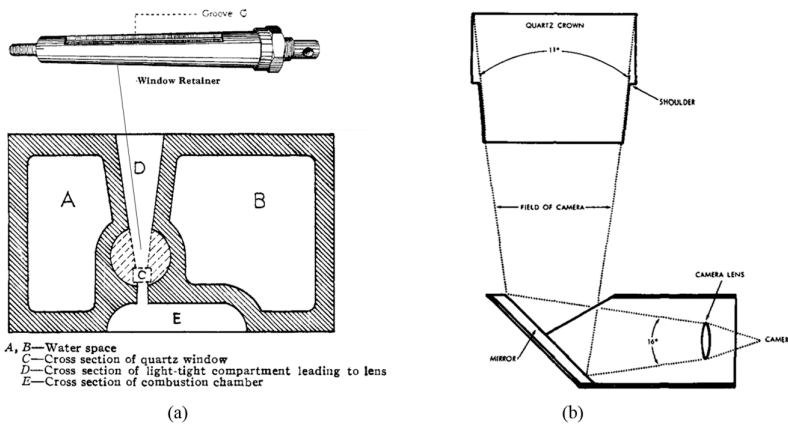


Figure 3.1: a) Cross section of the Withrow and Boyd cylinder head its the rotating window retainer. Reproduced from [64]. b) The principle of the optical access in the Bowditch quartz piston engine. Reproduced from [65].

With the introduction of overhead valves new approaches to the optical access was needed, which in 1958 lead to a breakthrough in optical engine design as Bowditch presented the quartz piston engine, today more widely recognized as the Bowditch design [65]. He also used the side view, but manufactured a hollow piston extension with a piston in quartz at the top hence allowing optical access from below, as shown in Figure 3.1 (b).

This brief history of the optical engine merely touches on the vast amount of systems that lead up to the optical research equipment we use today, but it pinpoints some of the important steps in its development.

3.1.2 Approaches in optical systems

To meet the diversity in research questions the optically accessible systems need specific designs. A combustion vessel or spray bomb is considered to be the most fundamental approach. Combustion vessels contains a controlled constant volume environment, allowing the researcher to test the most fundamental combustion phenomena, for instance the difference in the combustion modes of flame propagation and diffusion combustion as introduced in section 2.1. Constant-volume combustion vessels are designed to simulate engine conditions close to TDC. To reach the desired temperature and pressure, a combustible gas is ignited by a spark plug in the chamber. The combustion quickly increases the temperature and pressure, which is let to cool down to desired conditions. When reached, fuel is injected and react with the set conditions. [66, 67]. Injector spray diagnostics is also investigated in these types of vessels. A rapid compression machine (RCM) can be used to generate closer resemblance with an actual engine, mainly to investigate chemical kinetics and auto ignition [60]. This type of machine hence only considers the compression and combustion events. The initial conditions of temperature and gas composition is set, and autoignition is initiated due to a rapid compression stroke. The least intrusive approach to optical diagnostics is of the combustion in an engine is the usage of an endoscope, which in principle, only requires a drilled hole to the combustion chamber. The limitation in the field of view is considerable, hence the result may be inconclusive. The best compromise and most versatile approach is, the Bowditch optical engine.

3.2 Optical engine design and specifications

The Bowditch optical engine in this work is built on a Volvo heavy duty engine, with the specifications presented in Table 3.1.

The optical access is allowed to the combustion chamber from the sides through quartz

Table 3.1: Engine specifications

<i>Displacement volume</i>	2123 cc
<i>Stroke</i>	153 mm
<i>Bore</i>	131 mm
<i>Connecting rod</i>	255 mm
<i>Compression ratio</i>	16:1
<i>Number of valves</i>	4
<i>Swirl</i>	Close to zero
<i>Fuel system</i>	Delphi F2 common rail external pump
<i>Orifices</i>	6
<i>Nozzle diameter</i>	212 μm
<i>Umbrella angle</i>	150°

windows and from beneath through a quartz piston. Although the principle is simple, designing an optical engine requires careful consideration. Three key factors were in mind during the design: maintenance, versatility and robustness, all with their own subcategories. Only the general ones are discussed here.

Maintenance of an optical engine is of great importance due to many factors. Combustion often generates soot, especially spray driven combustion, thus it must be easy to clean the components. To achieve this is to use a drop down liner as introduced by Espey and Dec in 1993 [68], which means that the liner can be disconnect from the side window holder and lowered, which in turn exposes the optical piston as well as the side windows. Many research facilities use pneumatic or hydraulic installations to lift the liner up and down, to decrease the cleaning time even more, however the engine design in this work simply uses a manual lever. The window holder and drop down liner is shown in Figure 3.2 There are pros and cons with both approaches in initial cost and cleaning time. Building an optical engine with a production engine as a base immediately limits the space, hence extra consideration of the maintenance access has to be considered. To allow extra room for maintenance, the whole optical assembly is designed to hang from the cylinder head, thus the cylinder head supports are enabled to be moved away from the optical assembly. Figure 3.3, shows two designs with optical assemblies. The left image shows how the assembly is supported by pillars, thus limiting the access around the liner. To the right is the hanging assembly which allows more space. The hanging assembly also allows the piston and window holder to be interchanged without disassembly of any other engine part, which takes below one hour.

Versatility is accomplished with a modular approach, by using a standard 50 mm x 50 mm bolt pattern, on as many components as possible. This facilitates access from three directions by rotating the piston extension and/or the mirror. From a diagnostics point of view this merely rotates the recorded image, however the feature are mainly helpful in the

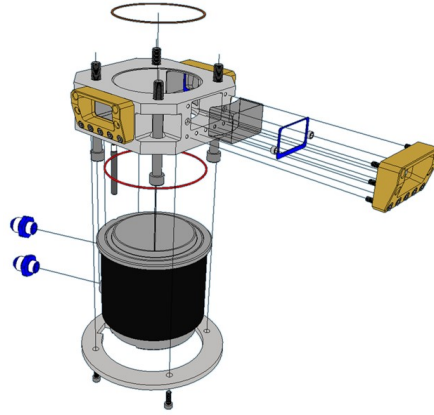


Figure 3.2: Exploded view of the window holder with the drop down liner.

logistics of placing the bulky diagnostics equipment around the engine.

The third design factor is robustness, and an optical engines are mainly limited by the optical liner. To facilitate high load operation, the side optical access was limited to a design with three windows, instead of the more fragile full quartz liner. Image of a CAD model of the set-up can be seen in Figure 3.2 and in 3.4.

Cylinder one is chosen as the operating piston to allow easy access. The remaining five cylinders pistons are fitted with tungsten weights for balancing the mass of the piston extension assembly, marked with red in Figure 3.4. The piston extension and the standard piston assembly act as a spring during operation, thus the squish height, which is the distance from the piston crown to the cylinder head, varies due to the deformation. Aronsson *et al.* did a detailed analysis of the compression of a piston extension with consideration of the actual change in the volume trace and consequently in the heat release calculation [69, 70]. Tests were performed both with static forces on the respective components and with optical diagnostics during engine operation. The results concluded that the large part of the increase in the squish height, originated from the standard engine components. To improve the stiffness of the piston extension of the engine designed in the current work, the extension cutout was redesigned. The new design in Figure 3.6 is inspired from the drop shaped form of the cutout designed by Toyota [71]. This design is only compressed 0.6 mm at 90 bar TDC pressure where the previous design was compressed 1.65 mm at 87 bar, as seen in Figure 3.5. A factor not to neglect is the difference in gas forces between combustion TDC and gas exchange TDC. Due to the higher inertia of the piston extension assembly the mass forces decrease the squish height. Thus it's important to always have a positive boost pressure in the inlet, to minimize the risk of failure due to collision with the valves

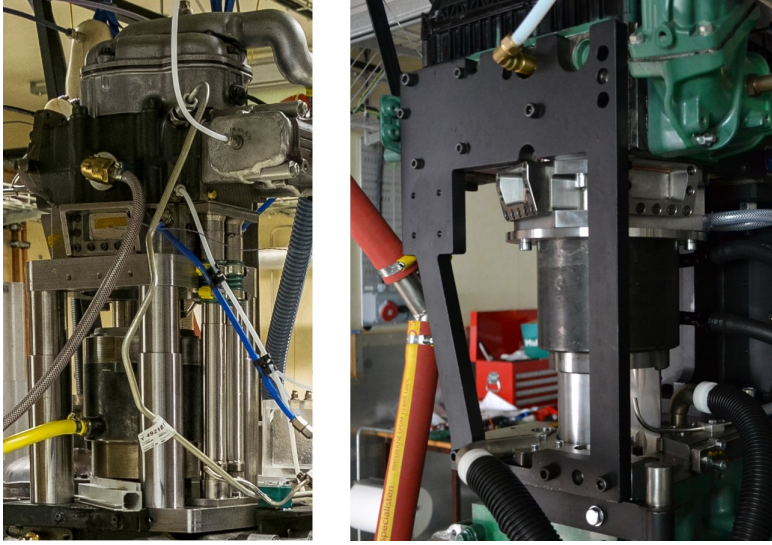


Figure 3.3: The left image shows a pillar design of an optical assembly. The right image shows the optical assembly hanging from the cylinder head.

or the cylinder head.

Since the Bowditch design does not allow a oil lubricated piston ring, an alternative solution with dry piston rings is needed. In this case the piston rings are made of Rulon J which is a PTFE compound enforced with glass fibres. The ring pack is self-lubricant and relies on the initial wear against the cylinder liner which adds a thin layer of the piston ring material onto its surface. Hence low friction and long durability is achieved. The ring pack consists of two compression rings, with supporting O-rings behind them and one guide ring mounted below the compression rings. Worth nothing is that the main use of this kind of piston rings are in dry or wet conditions, depending on material compound, and without combustion, hence the life span is quite drastically decreased in this application. The piston rings are mounted on the piston crown holder which is manufactured in titanium to avoid excessive thermal expansion of the material, respectively marked as 3-4 and 2 in Figure 3.6. The quartz piston crown with a shape based on the Volvo standard piston is glued onto the same titanium holder.

3.2.1 Limitations

Even though optical engines are valuable tools for detailed diagnostics, the modifications come with compromises and limitations. These are both due to material and mechanical

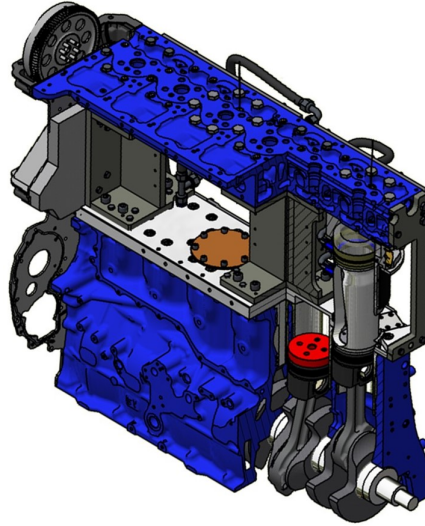


Figure 3.4: A two way cross section of the optical engine used in this thesis

properties. The quartz used for windows and piston has lower heat conductivity than the metal piston and liner. Due to this difference the quartz does not transfer heat as well as the metal which can result in earlier SOC due to higher surface temperatures [72]. One way to keep the heat from accumulating in the material is to run the engine in skip-fire mode, for example, only running one combustion cycle in ten motored cycles.

To avoid that piston rings pass over the junction between the drop-down liner and the optical liner, the piston rings must be mounted in a lower than normal position, during operation. Figure 3.6 illustrates the position of the piston rings. This lower position increases the crevice volume compared to an standard engine, thus both more UHC can be trapped and the compression ratio decreases. The quartz piston is also brittle, and to avoid the heavy piston assembly from hitting the valves during gas exchange the squish height needs to be increased. Consequently, the compression ratio is once more decreased. To compensate for these factors, increased boost and tuned inlet temperature is used to reach a similar gas density as the normal metal engine would reach at TDC.

An additional factor that separates the optical engine from a production engine is the dry piston ring pack. These rings, being made of a PTFE compound, lacks the stiffness and durability oil lubricated metal piston rings. Inevitably, this leads to an increase in blow by.

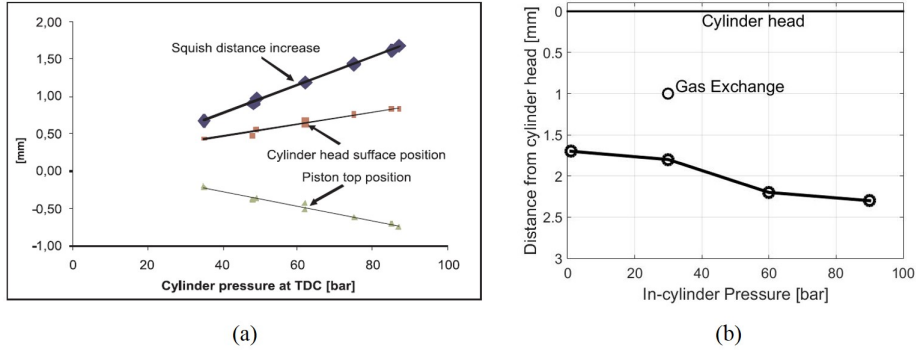


Figure 3.5: Comparison of the squish height of, a) the old piston extension from [69] and b) a new drop shaped piston design shape used in this work. Both compressions are optically measured at TDC at similar loads.

3.2.2 Auxiliary systems

To meet the operating conditions of an metal engine, the optical engine needs auxiliary systems to compensate for its low compression ratio and different in-cylinder thermal conductivity while operating under skip-fire. As the engine does not run continuously, no or very little exhaust produced. This means that there is no energy to propel a turbocharger nor any EGR to utilize.

For this reason the intake system is designed as described. The "EGR" in this system is produced in an external diesel furnace with stoichiometric combustion, producing no soot. Air is led through a flow meter before being mixed with the EGR. The mixture is compressed and cooled before being heated to a desired temperature.

An external Delphi fuel pump (F2R model) was used to reach the desired common rail pressure. All fuel pipes are made of PTFE or stainless steel to avoid contamination of the fuel entering the combustion chamber, which could introduce unwanted background noise in optical measurements.

3.3 Diagnostics

The experiments in this thesis are carried out with high speed video (HSV), planar laser-induced fluorescence (PLIF) and stochastic reactor model (SRM) simulations. The latter can be read about in Paper I.

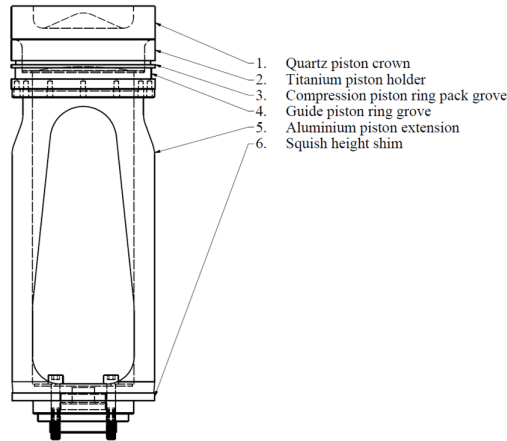


Figure 3.6: Drawing and description of the piston extension assembly. The piston crown depicted here was used in all experiments.

3.3.1 High speed video

Natural luminosity (NL) from the combustion chamber is recorded with a Photron Fastcam SA-X2 high speed CMOS camera positioned as in Figure 3.1, (b). The NL signal consists of radiation from glowing soot particles and chemiluminescence, that is, the light emitted naturally from the flame. Soot, or black body radiation, emit the highest intensity. The black bodies absorb and incandescently re-emits temperature-dependent broadband thermal radiation, as described by Planck's law. The chemiluminescence is due the chemical reactions that produce species in an excited state which radiates as they relax to the ground state. The emitted wavelength are species specific and it is thus possible to separate signals from different species by using filters, at least to some extent. The luminosity of the broadband radiation of soot does, however, make it difficult to separate the signals completely [73].

Line of sight techniques provide information from the whole combustion chamber volume, which must be considered when analysing the data. Laser diagnostics can be used to illuminate species outside the visible spectra, and provide with spatial information in 2D.

3.3.2 Laser diagnostics

Laser diagnostics are used to retrieve a detailed and species specific representation of the combustion process, by investigating temperature, velocity, fuel distribution and so forth. The diagnostic method in this work is, as mentioned, PLIF. As the name implies, this method requires that the laser beam is formed into a thin sheet, to provide only information

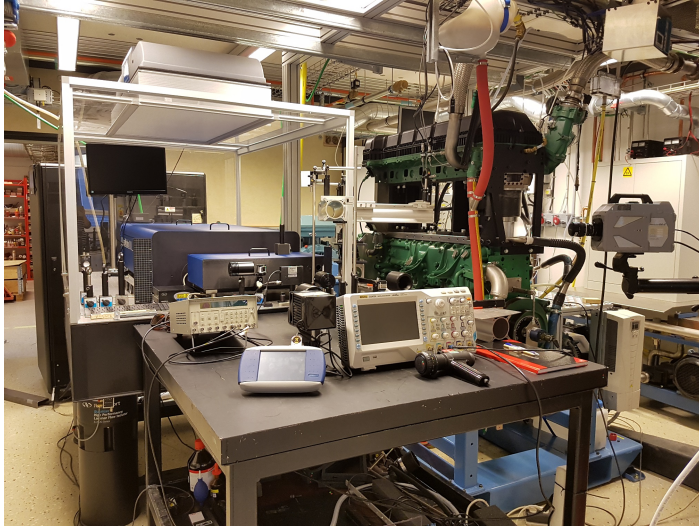


Figure 3.7: The research lab with high speed burst laser, optical engine and a high speed camera.

from a section through the combustion chamber volume. The HSV camera collecting the emitted light is placed perpendicularly to the sheet. Figure 3.7, shows the PLIF diagnostics system to the left of the optical engine. On the right hand side is the high speed camera that collects the images. In this image the laser is formed into a horizontal sheet and the camera images the signal from beneath via the 45-degree mirror.

Briefly described, the LIF is emitted from molecules that have absorbed photons from a laser. When they relax from the excited state to the ground state, they emit photons that make up the fluorescence. All molecules and atoms have their own energy levels, and depending on the laser wavelength, different species emit light accordingly, making the technique species-specific. Certain species are formed during the different stages of combustion, and can therefore be traced separately.

In this work the PLIF is used in tracing the fuel distribution under ultra-high speed conditions, during a cycle. Normal pump fuel normally contains a mixture of unknown components, making it difficult to determine which component the signal comes from. By using a single component non fluorescing fuel like iso-octane or n-heptane, and adding a fluorescent fuel tracer to it, the source of the fluorescence becomes known. In this work, 10% of acetone is added by volume to the fuel (PRF87, see section 2.4). Acetone has properties and behaviour similar to the single component fuels, which makes it a suitable tracer for this study [73] .

3.3.3 Heat release analysis

The heat release analysis provides a global representation of the combustion process. The data required for the calculations are collected using a pressure sensor located in the combustion chamber. The calculations are used as a tool to describe the combustion process and its parts, as previously described in Figure 2.2. The heat release either presented as an accumulated heat release, which represents the total energy produced up to a given time, or as a rate of heat release. This means that control parameters like the start of combustion (SOC), the point of 50% of heat released (CA₅₀), combustion duration among others can be extracted from the heat release analysis.

The heat release calculations used in this work are based on [2, 12]. Fundamentally, they are based on the first law of thermodynamics as in Equation 3.1, and they treat the combustion chamber as a closed system, neglecting the mass transfer over the system boundary, like the mass of injected fuel or the loss off fuel due to blow by in the crevice volume. Conditions in the system are considered as uniform in terms of pressure and temperature. The energy balance of the system is given by

$$\frac{dQ}{dt} = \frac{dU}{dt} + \frac{dW}{dt} \quad (3.1)$$

where dQ/dt is the heat added to the system, dU/dt is the change in internal energy and dW/dt is the rate of work. The equation needs to be formulated to fit the purpose of a combustion engine, thus being a function of volume and pressure. In order to achieve this the internal energy U can be formulated as

$$U = mC_v T \quad (3.2)$$

where m is the mass, C_v the specific heat of a constant volume and T the temperature of the system. Assuming a constant mass the derivative of the internal energy becomes

$$\frac{dU}{dt} = mC_v \frac{dT}{dt} \quad (3.3)$$

The temperature is obtained from the ideal gas law, meaning that we are assuming a homogeneous global temperature in the combustion chamber.

$$pV = mRT \quad (3.4)$$

where p , represents the pressure and the V is the volume. Assuming R to be constant, the internal energy can hence be expressed as

$$\frac{dU}{dt} = \frac{C_v}{R} \left(p \frac{dV}{dt} + V \frac{dp}{dt} \right) \quad (3.5)$$

The rate of change of work dW/dt , which is the second term in Equation 3.1, is defined as mechanical work

$$\frac{dW}{dt} = p \frac{dV}{dt} \quad (3.6)$$

The above derived Equations 3.5 and 3.6, is used in Equation 3.2 and is rewritten as

$$\frac{dQ}{dt} = \frac{C_v}{R} \left(V \frac{dp}{dt} + p \frac{dV}{dt} \right) + p \frac{dV}{dt} \quad (3.7)$$

Using the ratio of specific heats

$$\gamma = \frac{C_p}{C_v} \quad (3.8)$$

in combination with the expression of the gas constant

$$R = C_p - C_v \quad (3.9)$$

C_v/R can be written as

$$\frac{C_v}{R} = \frac{1}{\gamma - 1} \quad (3.10)$$

which simplifies the Equation 3.7 by replacing C_v/R , we obtain

$$\frac{dQ}{dt} = \frac{\gamma}{\gamma - 1} p \frac{dV}{dt} + \frac{1}{\gamma - 1} V \frac{dp}{dt} \quad (3.11)$$

The unit of interest when calculating the heat release is not time but crank angle degrees (CAD), θ , and 3.11 thereby becomes:

$$\frac{dQ}{d\theta} = \frac{\gamma}{\gamma - 1} p \frac{dV}{d\theta} + \frac{1}{\gamma - 1} V \frac{dp}{d\theta} \quad (3.12)$$

The heat release in Equation 3.12, does not include the heat transfer to the walls. By adding the estimation of heat transfer, assuming a uniform and constant wall temperature, the actual heat release from combustion can be calculated as

$$\frac{dQ_{HT}}{dt} = hA(T - T_{wall}) \quad (3.13)$$

where A_{wall} is the wall area, and T_{wall} is the wall temperature. h is the heat transfer coefficient, empirically derived by Woschni [2]

$$h = 3.26B^{-0.2}p^{0.8}T^{-0.55}w^{0.8} \quad (3.14)$$

where B , is the cylinder bore and w a characteristic speed

$$w = C_1 S_p + C_2 \frac{V_d T_r}{p_r V_r} (p - p_m) \quad (3.15)$$

where C_1 and C_2 are constants that are tuned to the specific engine. S_p represent the mean piston speed and V_d the displacement volume. The factors T_r , temperature, p_r , pressure and V_r , volume are the conditions at a reference point, e.g. the conditions at inlet valve closing (IVC). $p - p_m$ is the difference between a combustion cycle and a motored pressure trace. Finally, the heat release equation is derived as

$$\frac{dQ}{d\theta} = \frac{\gamma}{\gamma - 1} p \frac{dV}{d\theta} + \frac{1}{\gamma - 1} V \frac{dp}{d\theta} + \frac{dQ_{HT}}{dt} \quad (3.16)$$

As described above the calculations are made with several assumptions and simplifications, hence the information obtained is not completely accurate. Also neglected in this calculation is the earlier described changes in the volume trace due to deformation of the piston assembly [69, 70].

After discussing the setup, we will move on to results in the next chapter.

Chapter 4

Results and discussion

The results in this chapter are organized according to the transition between the combustion modes, going from HCCI via PPC to diffusion combustion. The chapter is divided into two main categories; the first addressing the kinetic combustion modes and the other addressing the diffusion combustion. The first part focuses on the lower to intermediate load regimes, in the HCCI and PPC modes. The main interest lies in the combustion characteristics and sources of UHC, which is a known problem in LTC (see section 2.3). The second part moves into the high load regime where diffusion combustion is utilized, addressing the correlation between LoL and soot reduction by using gasoline as fuel compared to diesel.

4.1 Kinetically controlled combustion

This section revolves around kinetically controlled combustion modes. The covered loads are from 7 bar IMEP_g up to 12 bar IMEP_g, which is relatively low for a heavy duty application. Through the load steps, different kinetic combustion modes have been utilized, from HCCI, via PPC, to the intermediate load step where the process partly begins to involve diffusion combustion.

4.1.1 HCCI

The initial step in the transition between combustion modes is HCCI. This is part of the work in Paper II, where an analysis of how the sensitivity of combustion stability to the level of fuel and air premixing, and bulk temperature varies between HCCI to PPC.

The analysis was carried out by running the engine in skip-fire mode with three consec-

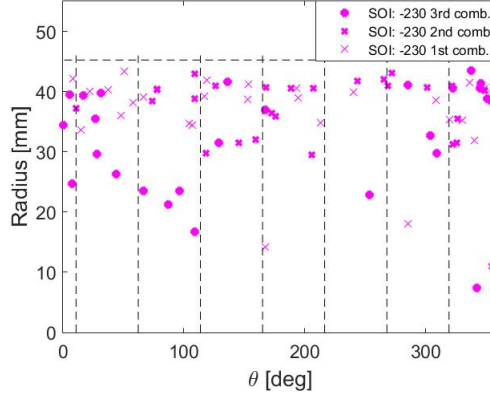


Figure 4.1: Radial and angular position of the SOC in relation to the injection nozzle. The labels; 1st, 2nd, 3rd corresponds to each cycle in the cycle-to-cycle temperature sweep. The horizontal dashed line represent the piston bowl rim, and the vertical dashed lines the injector nozzle holes trajectory.

utive combustion cycles followed with ten motored cycles. With this approach the initial conditions of the first combustion cycle is equal to the inlet conditions. In the following two cycles, residual gases and heat from the preceding cycle, are trapped in the combustion chamber. This leads to a temperature increase from one cycle to the next. Thus a method to evaluate the sensitivity of combustion stability correlated with initial combustion location, as a function of fuel and air premixing, and bulk temperature was developed.

High speed imaging of in-cylinder chemiluminescence was performed to determine the location of the first ignition kernel in the combustion chamber, Figure 4.1 shows the result. The y-axis represent the radial distance from the injector tip, and the x-axis the angular position. The vertical dashed lines represent the spray trajectories and the horizontal corresponds to the piston bowl rim. Each marker results from a single combustion cycle.

In the first combustion cycle (1st comb.) in Figure 4.1, the change shows a tendency to ignite at the periphery of the piston bowl, which indicates that the local temperature is higher close to the piston rim and squish regions. These finding are in line with the work of [34, 35]. This can partly be explained by hot gases escaping the squish volume, igniting the accumulated air and fuel mixture inside the piston bowl. For the 2nd and 3rd combustion cycles the initial combustion location tends to move away from the bowl rim as the global bulk temperature increases with the residual gases from the preceding cycle.

The NL images sequence in Figure 4.2, shows the combustion closest resembling the mean pressure trace presented in the top image. The image acquired, at 3.4 CAD aTDC confirms that the first kernel appears at the piston bowl periphery. In the following two images, 4.4 and 5.4 CAD aTDC, the combustion rapidly continues as a sequence of autoignition along the bowl periphery in both directions. At the same time, combustion proceeds into the bulk

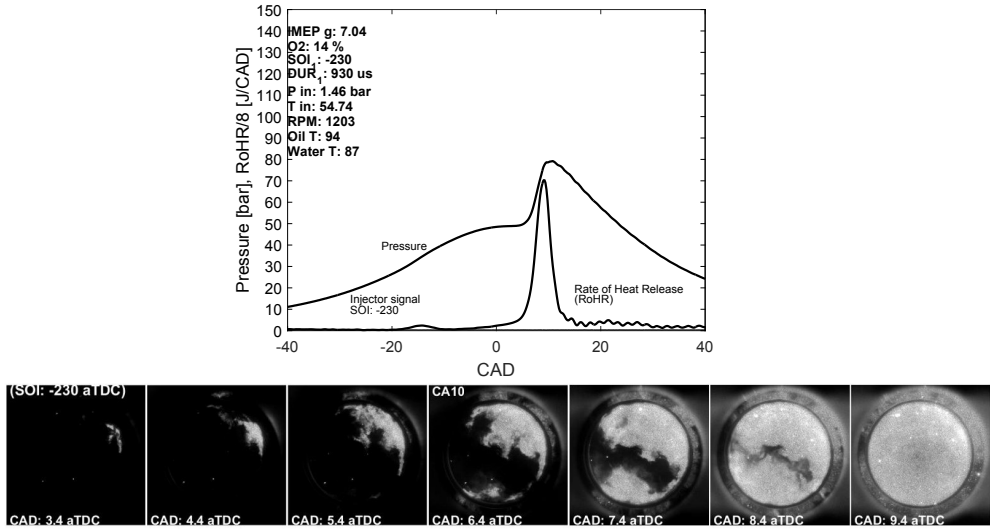


Figure 4.2: Typical combustion progress in HCCI, with pressure trace and heat release complemented with images obtained through the piston-crown window.

of the combustion chamber, followed by new ignition kernels appearing at 6.4 CAD aTDC (CA₁₀). The new kernels are likely to be ignited due to the increase in bulk temperature. After this the combustion is rapid, reaching the peak heat release at approximately 9.4 CAD aTDC as the full bulk of the combustion chamber is ignited.

There is no swirl induced in the combustion chamber in these experiments, which is also evident in the HSV images. Turbulence, is mainly generated by the injection and in the squish region, where the latter is the only source present at the start of HCCI combustion.

HCCI is well known for having limitations in both controllability and high pressure rise rate, hence the trends has moved to injection strategies more closely coupled to the combustion. The following section shows the transition, going from a homogeneous combustion to a more stratified one.

4.1.1.1 Transition from HCCI to PPC

SOI was swept from -230 to -13 CAD aTDC to study the transition from HCCI to PPC conditions. At each SOI timing, the three first fired cycles represent a "sweep" in in-cylinder temperature. The results from the transition helps us to further understand the sensitivity of combustion stability and the correlation to bulk temperature and the premixing of the fuel and air charge. No injections were made between -230 and -28 CAD aTDC, to avoid injecting into the squish region, wall wetting and trapping in the crevice volume [74, 75].

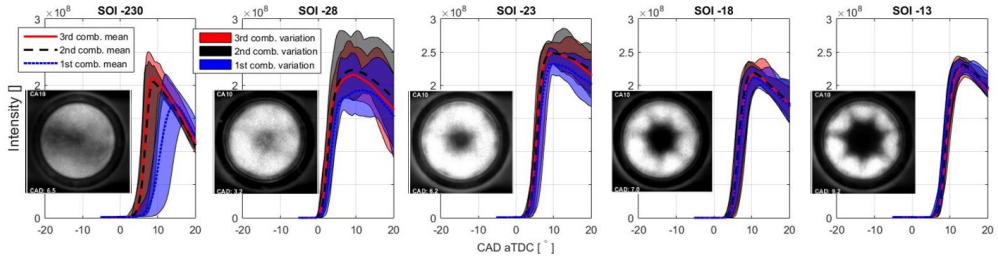


Figure 4.3: Each case represent the transition stages from HCCI (SOI -230 CAD aTDC) to PPC. The mean intensity signals are retrieved from three continuous combustion cycles under skip fire operation; 3 combustion cycles and 10 motored. The fields represents the spread in intensity from due to cycle to cycle variation. The images are the average representation of each combustion mode at CA10.

Figure 4.3 presents the sensitivity analysis during the mode transition. HSV imaging was used and the mean intensity of the NL represents the combustion, as it has been shown to correlate with the heat release rate [76]. Each sub-figure displays the combustion progress at each step of the transition. The lines are the mean NL intensity for the three consecutive cycles at the beginning (comb. mean). The surrounding color fields are the spread from cycle-to-cycle (comb. variation). HSV images are the means of multiple cycles to emphasize the characteristic appearance at CA10.

HCCI (SOI -230), in Figure 4.3, which is homogeneous, or close to homogeneous, shows low variation in the combustion intensity, especially for the second and third cycle with higher in-cylinder temperature. The first cycle shows high sensitivity to the temperature, as it is both retarded and shows larger cycle-to-cycle variations compared to the following cycles.

Moving into the PPC region, here represented by SOI -28 CAD aTDC, which is the most premixed case with fuel injected inside the piston bowl. As seen in Figure 4.3, a large spread in combustion intensity is seen from cycle to cycle, thus indicating a stochastic mixing behaviour. The combustion phasing sensitivity does, however, begin to be less prominent, as the mean intensity curve from the first combustion (1st comb. mean) is closer to the second curve (2nd comb. mean), indicating richer conditions at the start of combustion. The trend continues as SOI is retarded to -23 CAD aTDC, which accordingly display less spread in the mean intensity and less temperature dependency. Although, retarding an additional 5 CAD, there's a drastic decrease in the sensitivity.

At SOI -18 CAD aTDC, in Figure 4.3, uniform combustion areas appear, divided by the wakes of the injected fuel jets. While the stratification increases the variation in intensity decreases, so does the sensitivity to temperature variations. These trends get even more prominent with SOI of -13 CAD aTDC. There are now multiple uniform combustion areas, which all are prone to ignite.

The trends can also be seen in the location of the SOC kernels in Figure 4.4. Like the

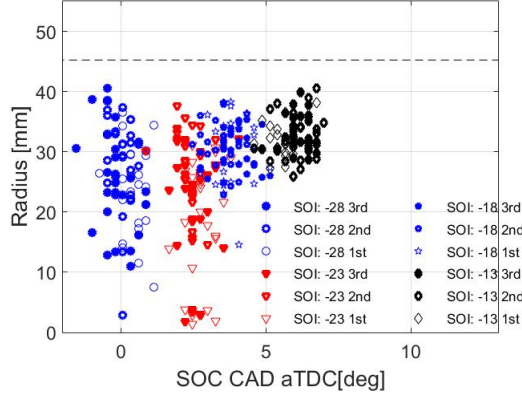


Figure 4.4: Radial location of the first visible combustion NL, as a function of SOC. The y-axis corresponds to the radial distance from the injector tip. The labels; (1st, 2nd and 3rd) corresponds to each cycle of the three first combustion cycles, where the first follows a sequence of motored cycles. The horizontal dashed line represents the location of the piston bowl rim.

previously described HCCI case in Figure 4.1, this figure represents the radial distance of the first visible combustion kernel from the injector tip as a function of SOC. Each marker represents the first visible kernel in the combustion chamber, for each SOI and in the 1st, 2nd and 3rd consecutive combustion cycles. Here, it is clear that the mixing process prior to combustion is highly related to the stochastic behaviour of the combustion intensity and consequently the heat release.

For both the earlier SOI strategies of -28 and -23 CAD aTDC, the radial location of combustion appears stochastic, similar to the trend with the intensity in Figure 4.3. This can be explained by the HSV images in the same figure, as premixing being too short for the fuel and air to reach one homogeneous mixture as for the SOI -230, and too long to maintain the uniform stratified fuel areas for SOI -18 and -13. This leads to an irregular behaviour of the combustion. Shifting SOI from -23 to -18 CAD aTDC, the stochastic behaviour rapidly disappears.

This can possibly be explained by a geometrical effect, as the injected fuel impinges the piston bowl wall at different heights. The bowl shape can be seen in Figure 3.6 in section 3.2.1. Based on the work by [74], the earlier injection at -23 CAD aTDC impinges higher on the piston bowl wall and a clockwise vortex appears as fuel travels downward and inward towards the piston bowl center. For the later injection case of -18 CAD aTDC the injection impinges the piston bowl at a lower point, thereby the fuel trajectory will be upwards in a counter clockwise vortex along the bowl wall, causing the fuel vapour to tumble in a tighter radial band. However, the narrow band may merely be an effect of the ignition delay, meaning that the fuel and air mixture reaches a temperature prone to autoignition faster than the advanced injections.

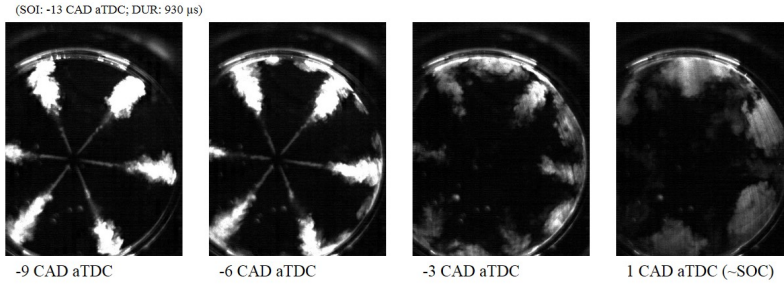


Figure 4.5: Fuel-PLIF of single injection PPC. Excited deep in the piston bowl, 12mm from the cylinder head. The four images represents the relevant stages of the fuel distribution process prior combustion. The last image contains the fuel distribution just before combustion commence, which is seen in Figure 4.6.

Reaching SOI -13 CAD aTDC the radial band shrinks even more. This is a typical PPC case, with an injection that ends before SOC and a uniform partially premixed charge in the combustion chamber.

The single homogeneous region of the HCCI case has now been divided into several uniform combustion regions, with lower sensitivity to temperature and higher controllability with the closer coupling of SOI and SOC.

4.1.2 PPC

This section is based on Paper II, III where PPC was used as a baseline case.

Figure 4.5 contains fuel tracer PLIF of the single injection PPC case with SOI at SOI -13 CAD aTDC. The chosen images are typical fuel distributions at different stages of the cycle. The laser sheet is placed 12 mm from the cylinder head, thus the sheet more or less touches the piston bowl pip at TDC.

At -9 CAD aTDC the vaporized fuel jet impinges on the piston bowl wall, spreads in opposite directions along the wall. -6 CAD aTDC shows the onset just before EOI. The edge of the adjacent jets breaks into small counter rotating vortexes, before mixing in the next image.

In the image taken at -3 CAD aTDC, the small counter vortexes breaks up into larger eddies, as the remaining inertia in the fuel jet is fed into it. The fuel vapour wedged in between the spray trajectories is forced to recirculate into the combustion chamber center, initiating the formation of uniform, fuel rich pockets. Finally, these pockets autoignite after 1 CAD aTDC in Figure 4.5. Each fuel pocket is split by the upstream fuel jet trajectory which remains after EOI. Some fuel remains in the wake of the fuel jet, and a signal can also be seen in the central region of the piston bowl.

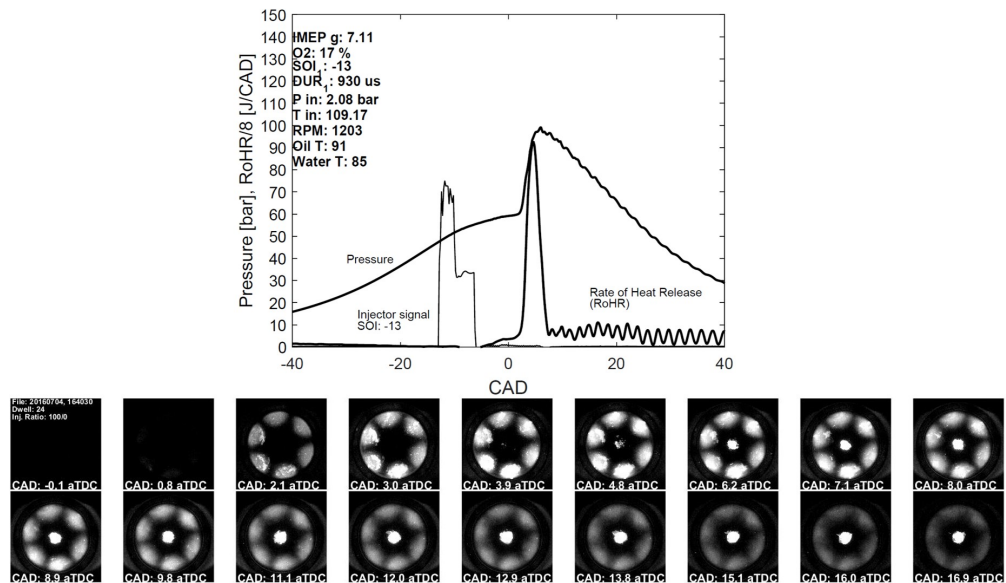


Figure 4.6: Typical combustion progress in PPC, with pressure trace and heat release complemented with images obtained through the piston-crown window.

When a combustible mixture is obtained, the NL of the combustion becomes visible in the recirculated part of the fuel jet, as seen in the image acquired at 2.1 CAD aTDC in Figure 4.6. The images presented are mean HSV frames from 35 cycles of combustion. Also presented in the figure is the corresponding pressure trace and heat release. The initiated combustion in image 2.1 CAD aTDC is somewhat misleading, since combustion normally starts in one of the uniform fuel areas, and then followed by the six other fuel pockets igniting shortly thereafter. As the combustion progresses, the combustion areas grow rapidly inwards where they level out as the main heat release peaks, as seen in Figure 4.6. Later, the recirculated combustion areas slowly shrink and fade out to the piston bowl wall until no signal is detected. During the combustion, the signal in the center of the chamber appears close to zero indicating overly lean conditions, as discussed by, [52, 46] and also seen in the PLIF image in Figure 4.5. Hence this area is a probable source of UHC, due to incomplete combustion.

UHC and CO are both significant emissions for PPC conditions. The main sources are trapped fuel in the crevice and squish region, rich areas due to injector dribble in the middle of the combustion chamber, and also lean regions [47, 48]. As will be discussed below, post injections is a potential means to reduce emissions related to these regions.

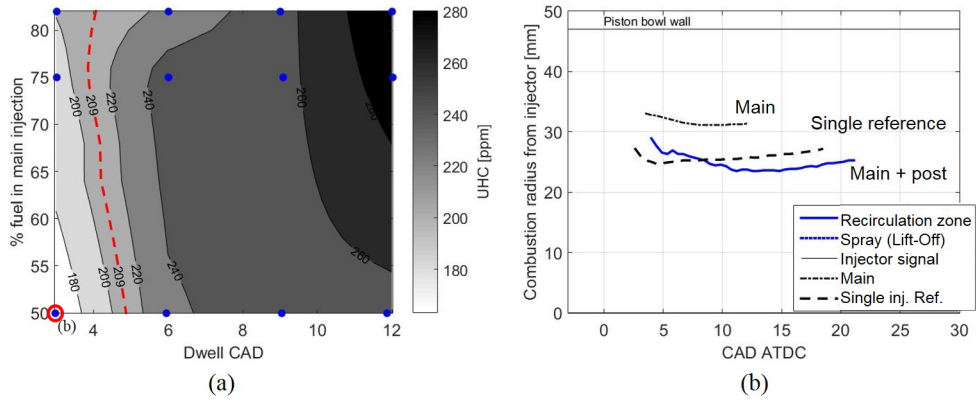


Figure 4.7: a) Unburned HC as a function of the separation between main and post injection (dwell), and the ratio of fuel mass between the main and post injection. Blue dot represent the experimental measurement points. The dashed red line represent level of the single injection base line case. b) The combustion radius of single and post injection strategies. The legend describes the

4.1.2.1 Post injections

Using post injections has been shown to reduce the UHC under for low load diesel PPC conditions, and implied that these reduce UHC stemming from the central region of the piston bowl [52, 51]. This section presents the results of post injections applied in an attempt to reduce UHC emissions. The same gasoline PPC case as presented previously in section 4.1.2 is used as a reference case. Emission measurements and HSV imaging was carried out simultaneously, while load and the start of the main injection was maintained constant. Dwell and repartition of mass between the main and post injections were varied to evaluate their effect.

Figure 4.7 shows the UHC emissions as a function of the dwell and fuel mass repartition. Dwell is here defined as crank angle interval between the falling edge of the main injector actuation signal and the rise of the post injection signal. The repartition is defined as the ratio between the durations of the two injector signals, which may not exactly correspond to the repartition of the actual fuel mass.

The first observation in Figure 4.7.a is that the UHC is clearly more affected by the dwell than the fuel injection ratio. The lowest UHC emissions are found in the strategy with two equally sized close coupled injections (From here on called D50.3, where D is merely a letter to separate the cases, 50 refers to the 50% repartition between the two injection signals to the 3 is 3 CAD dwell). The cases with a small post injection shows the highest emissions.

A post injection with EOI after SOC was tested with the ambition to enrich the central region close to the nozzle. It proved not to be successful, due to the high resistance to auto-

ignition of PRF87. Either the post injection becomes too large, and resulting in combustion in the outer region of the piston bowl, or too small, where conditions become too rich due to low momentum in the jet, hence the fuel won't mix sufficiently with air prior to combustion of the post injection.

Figure 4.7.b shows the mean radial distance from the injector to the closest NL of the uniform combustion areas. The D50.3 case is presented. Three curves are shown: the single injection reference, which corresponds to the case described above in 4.1.2; the main, which is the combustion from the main injection only; and main + post which accordingly corresponds to the double injections. The case presented in Figure 4.7.b is marked with a red circle in Figure 4.7.a.

The results in Figure 4.7.b show how the radius of D50.3 is reduced downstream in the recirculated area. The combustion radius also remains more stagnant than the single reference case, hence enclosing the lean region for a longer duration. This can possibly be explained by the hypothesis of O'Connor *et al.*[52], where the post injection acts close enough to the main injection to push the fuel and air mixture downstream the recirculation zone and towards bowl centre. Even so, two needle lifts cause both more throttling of the fuel jet and one additional entrainment wave between the main and post injection, which in turn may decrease the jet velocity and stagnate the jet. The main injection in Figure 4.7.b appears at the the combustion chamber periphery and does not contain momentum enough to reach back into the central regions of the combustion chamber.

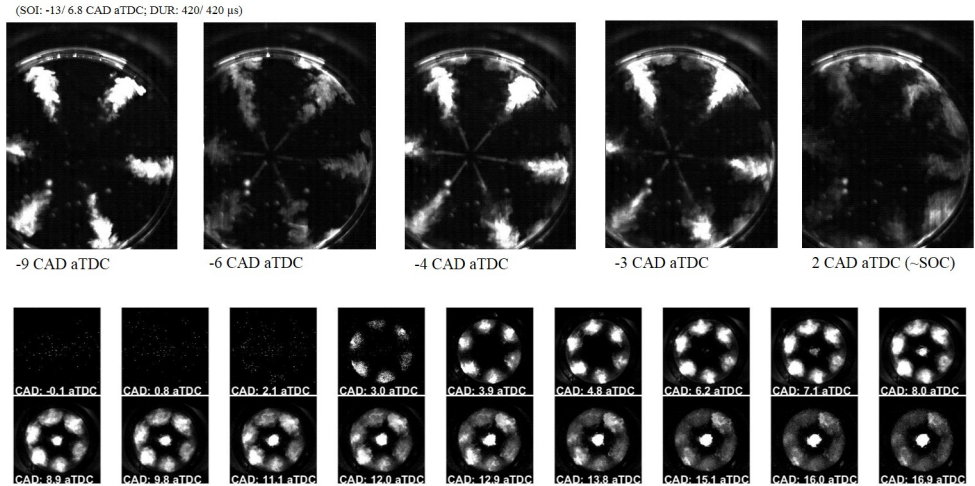


Figure 4.8: The top row includes the fuel-PLIF of with main and post injection PPC. Excited deep in the piston bowl, 12 mm below the cylinder head. The five images represents the relevant stages in the fuel distribution process prior combustion. The bottom row shows the NL images of the main and post injection combustion.

Fuel-PLIF was used to gain further insight. Looking at the fuel-PLIF images in the upper

row in Figure 4.8 it's observed at -9 CAD aTDC that the main injection does not reach the piston bowl wall before EOI. Only the remaining momentum of the injection transports the fuel from that point on. In the image of -6 CAD aTDC, the post injection has just been initiated (SOI: -6.8 CAD aTDC). Furthermore, the stagnation of the main injection becomes clearly visible in this image. The post injection quickly penetrates the wake of the main injection. Noteworthy here is that the second injection reaches the bowl wall faster (travel duration of 3 CAD) than the main injection (travel duration of 4 CAD).

This phenomenon may be due to the entrainment wave of the main injection. As the post injection starts it gets pulled along the wake flow, or slipstreaming, thus reaching the wall at greater speed. It should not be neglected that this may potentially be an effect of hydraulic oscillations in the fuel rail. Nevertheless the fuel reaches the bowl wall before injection ends as seen at -3 CAD aTDC. At this stage, the fuel from the post injection quickly travels along the bowl wall, and seemingly catches up with the main injection before mixing with the adjacent fuel jet. Prior to SOC at 2 CAD aTDC there is still fuel lingering upstream in the fuel jet, in contrast with the single injection case in Figure 4.5 where most fuel reached the recirculation zone at 1 CAD aTDC at SOC.

The lower two rows in Figure 4.8 contain an averaged HSV sequence of the same case. At 3 CAD aTDC the fuel autoignites close to the bowl rim, which is in line with the fuel-PLIF results. As combustion progresses, the areas grow inwards. In these areas a mushroom shape with its root against the bowl wall appears with higher intensity than the areas around it. These shapes are due to the remaining inertia from the post injections that collide and generate two large counter-rotating vortices.

This shows that using close coupled double injections, the post injection reaches a higher jet velocity in the wake flow of the main injection. This allows the fuel to reach further downstream into the recirculation zone, thereby enclosing the remaining over-lean area in the center of the combustion chamber, and possibly consuming the UHC. The double injection also has a shorter ignition delay which, together with the remaining turbulence, prolongs the combustion, giving less time for fuel and air to reach over-lean conditions.

Moving up in load, the PPC is not suitable due to the rapid heat release rate. For this reason strategies where the energy released is distributed more preferably are more preferable.

4.1.3 Intermediate

The next transition stage applies as load is increased, in this case to 10 bar IMEP_g. The combustion process now enters an intermediate stage between kinetic combustion (such as PPC) and diffusion combustion. The combustion still shows a high peak heat release due to substantial premixing, but is followed by a tail due to a small spray driven part, as seen

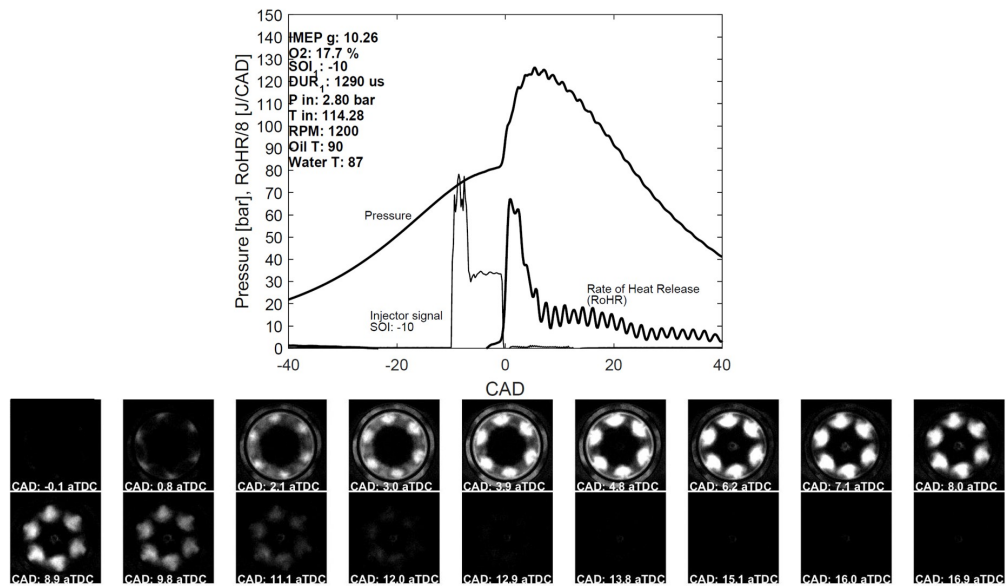


Figure 4.9: Typical combustion progress in the intermediate load between PPC and diffusion combustion, with pressure trace and heat release complemented with images obtained through the piston-crown window.

in the top sub-figure in Figure 4.9.

As seen in the mean HSV images, the auto ignition occurs in the premixed recirculated zones at 0.8 CAD aTDC, just as in the lower load cases. This means that the jet has impinged on the bowl wall and started to recirculate, in similar manner as presented for PPC in Figure 4.5. A weak NL signal from the leading edge of the fuel jet travelling on the piston bowl floor is seen in the same image. However likely, it can only be assumed that the fuel travel in this way due to the limitations of the line of sight technique.

The injection signal ends at TDC. Based on observations of the PLIF cases, it is safe to assume that the injector needle remains open for approximately 2 CAD after EOI. At 2.1 CAD aTDC the injection has ended, thus only the inertia remaining the gas drives the diffusion combustion. This is seen as the tail in the heat release trace in Figure 4.9, which quickly decay as the injection ends. A weak NL signal indicating the presence of an established LoL can be seen 2.1 and 3.0 CAD aTDC, in Figure 4.9. The remaining part of the fuel continues to feed the combustion areas in the periphery of the piston bowl, forming mushroom-like areas as the two adjacent, backwards-rotating fuel jets collide.

The backwards-rotating vortexes continues as combustion progresses and slowly fades out. This slows the combustion rate as well, which has a negative effect on efficiency since the effective expansion ratio decreases. The loss in momentum after EOI, may be an important factor as it decreases the mixing rate of fuel and air. Turbulence and/or swirl are effective

means to increase the mixing rate, even though swirl, has been shown to increase the heat losses through convection [2].

Different methods of generating turbulence can be applied, either swirl initiated in the intake, turbulence generated by the injected fuel jet, or by combustion chamber shapes like the piston bowl.

4.1.3.1 0-D simulations

Numerical simulations with a stochastic reactor model (SRM) were used in Paper I in a parametric study of the mixing intensity throughout the combustion.

The model, which is a 0-D model, relies on probability density functions (PDF) to determine the mixing and combustion progress. The PDF describe the probability for one molecule to react with another. Based on this chemical composition and the temperature at reaction are calculated. The model thereby doesn't contain any information about the spatial distribution of the molecules.

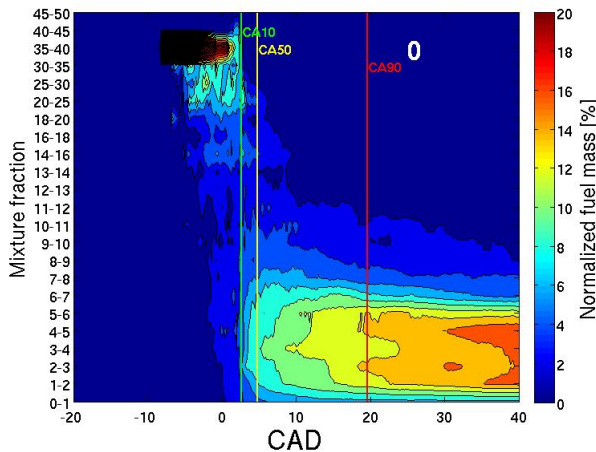


Figure 4.10: Fuel distribution in terms of mixture fraction, high values being rich. Where 4-5 correspond to stoichiometric conditions.

The presented reference case is similar to the one described above. The differences lie in the octane number, which was 91 instead of 87, thus yielding a longer ignition delay, and in a higher compression ratio, since the simulated case was of a metal engine. These two parameters compensate each other to some extent, since the optical engine used a lower compression ratio, but also a lower octane fuel.

Figure 4.10 describes the normalized fuel mass distribution in mixture fraction zones per

CAD, where higher values means richer conditions, as described in Equation 4.1.

$$\text{mixture fraction} = \frac{m_{\text{fuel}}}{m_{\text{fuel}} + m_{\text{oxidizer}}} * 100 \quad (4.1)$$

Stoichiometric conditions are found at a mixture fraction of 4.5(10). Vertical lines are set as markers for where the CA10, CA50 and CA90 occurs. The presented reference case (o), corresponds to the experimental data presented in Paper I. Heat release rates and the mixing intensity curves are found in Figure 4.11, which will be explained later. Figure 4.10 shows how the fuel is injected under rich conditions at mixture fractions of 35-40, and mixes with the ambient air. The fuel quickly mixes to leaner conditions, due to the turbulence caused by the spray. The SOC occurs around 0.2 CAD aTDC. At this stage the injection is nearly over, but there is still approximately 20 % or more fuel left in the rich zones. With the EOI the mixing intensity decays, which also was observed in the HSV images in Figure 4.9 of the parent section. In Figure 4.10, this can be seen as fuel being trapped in richer zones (mixture fractions ranging from 12-13 to 6-7) between CA50 and CA90 and thereafter, which can contribute to UHC emissions.

To alter this behaviour, the mixing intensity needs to be increased. For this reason a parametric study of the mixing intensity was performed. By altering the input mixing times to the model, ideas of which mixing parameter affects combustion output, could be generated. Indeed, when isolating factors in the way described below, their real effects are to some extent avoided, since changing one mixing parameter normally would affect the whole sequence. Even so, the presented result indicates the effect of each parameter.

The left column of Figure 4.11, shows the mixing time τ alteration, and the corresponding heat release result. The purple line represents the injected fuel mass, hence the curve is retarded compared to the signal in Figure 4.9. The right column in Figure 4.11 shows the resulting fuel distribution as earlier described.

The first row (B_{τ}) can be interpreted as mixing due to injection pressure, where the black curve (-1) shows the effect of increased injection pressure compared with the reference (o, Figure 4.10). Higher mixing of the injected fuel, increases the premixed heat release and the tail of the heat release decays more rapidly. In Paper I, the cumulative mass fraction burnt (MFB) is presented. For this case, the cumulative MFB increases with 1% to 95%, compared with the reference case. This can be explained with the fuel distribution. In the case of increased mixing of the injected fuel (B_{τ}) in Figure 4.11, right column, less fuel appears in the rich zones of mixture fractions of 11-12 compared to the reference case in Figure 4.10. After CA90, the majority of the remaining fuel is located in stoichiometric (mixture fraction 4-5) or leaner conditions.

The center row, C_{τ} , is the mixing at the onset of combustion, as seen in Figure 4.11. These

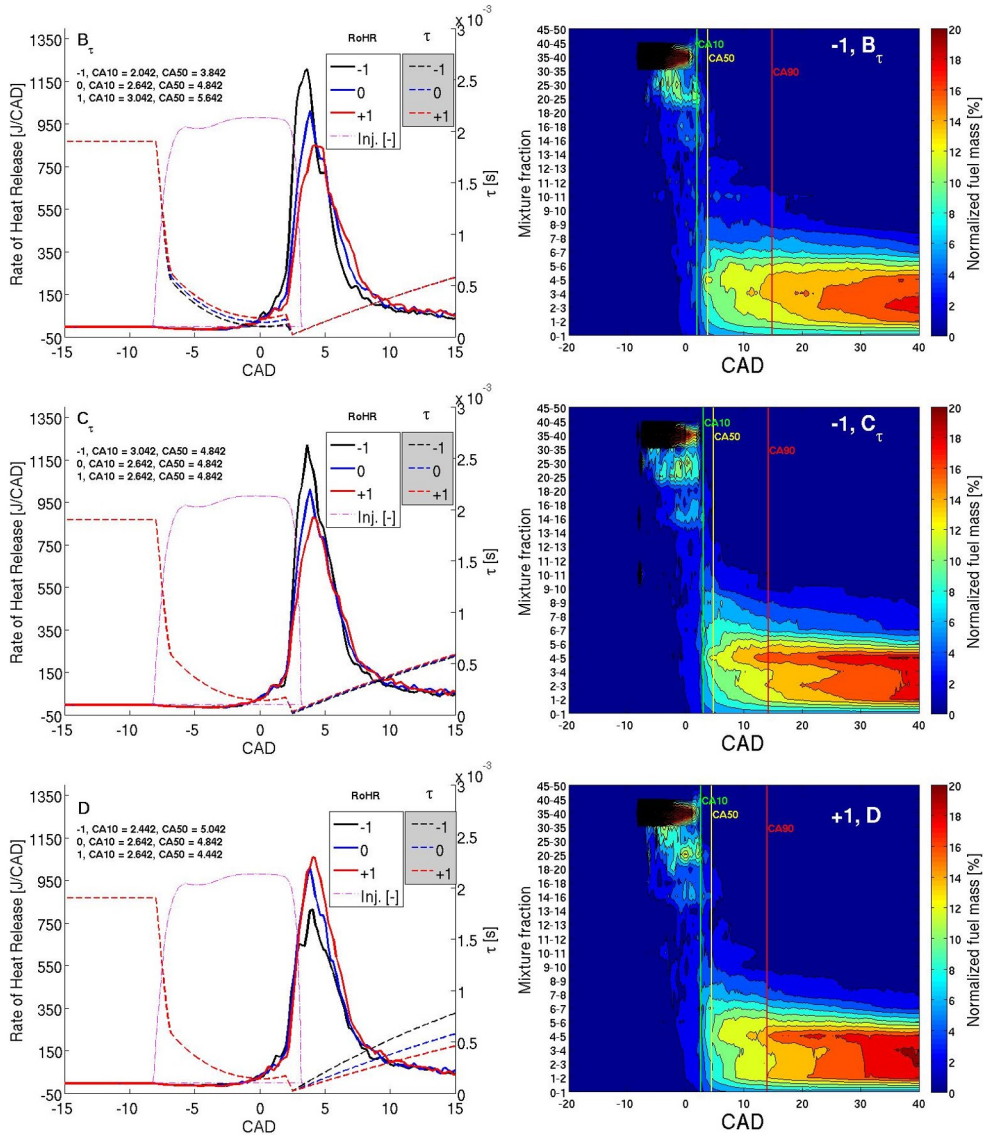


Figure 4.11: The left column shows the heat release rates and the mixing time curves. The right column describes the fuel distribution in terms of mixture fraction as a function of CAD. 4-5 correspond to stoichiometric conditions.

cases can also be seen as a parallel events with the fuel impinging on the piston bowl wall, and mixing with the adjacent sprays. The increase in mixing compared to the reference increases the cumulative MFB to 95%. As seen in the heat release, the peak increases due to the rapid mixing at SOC. The fuel distribution plot shows how a higher percentage of the fuel is closer to stoichiometric conditions around CA50. As combustion progresses, some fuel mass remains in richer zones after the CA90 marker, but the majority of the fuel is

concentrated to stoichiometric or lean zones.

The last row in Figure 4.11 shows the alteration of mixing intensity during combustion and expansion (D), meaning that the effect is studied after SOC. Here, +1, is the increased mixing factor, and should not be confused with the previous cases, where -1 has the highest mixing intensity. D has a stronger impact on the cumulative MFB than C_T , as it increases to 96% with an increased mixing (+1). This is partly reason is because the D parameter affects the whole expansion phase. As the mixing intensity is maintained after SOC, more fuel is mixed into combustible regions during the initial stages of combustion. The response to changes in D tells us that a higher mixing intensity during combustion and expansion would be preferable as the combustion efficiency (cumulative MFB) increases without affecting the pressure rise rate.

In a real engine, the turbulence and mixing phenomena are highly complex, and the alteration of one parameter would of course affect the turbulence in all steps. These numerical simulations show that the oxidation is an important factor, and that a preserved mixing intensity throughout the cycle clearly increase the combustion efficiency. This can be achieved with piston designs [77], which also will affect the C_T factor as fuel impinges on the piston. Swirl may also be used, but it will affect the whole combustion process from a more global perspective.

Higher turbulence normally leads to faster premixing of fuel and air, followed by high pressure rise rates for premixed combustion concepts. Increasing the octane number even more with ethanol enhances these trends even more. Ethanol has a RON number of 107 and is a highly volatile fuel. Thus longer ignition delays are to be expected, in combination with fast mixing with the ambient air. These properties lead to high pressure rise rates, but by utilizing pilot injections, the issue can potentially be suppressed.

4.1.3.2 Pilot injections

This section is based on Papers V and VI, where the intermediate load has been investigated with ethanol as fuel. Ethanol has been shown to be a contender as a possible PPC fuel, displaying even higher efficiencies and close to zero soot emissions. On the other hand, limitations are found in controllability and high peak pressure rise rates due to the high octane number fuel. These are mainly due to too long premixing. Likewise, controllability issues can be due to late injection timings when misfire is likely to occurs. Injection strategies are possible tools to meet the limitations.

These experiments were conducted in a single cylinder heavy-duty Scania D13 engine. The big differences to the Volvo MD13 engine are the utilization of swirl and the piston geometries. The work was made at the load of 12 bar IMEP_g.

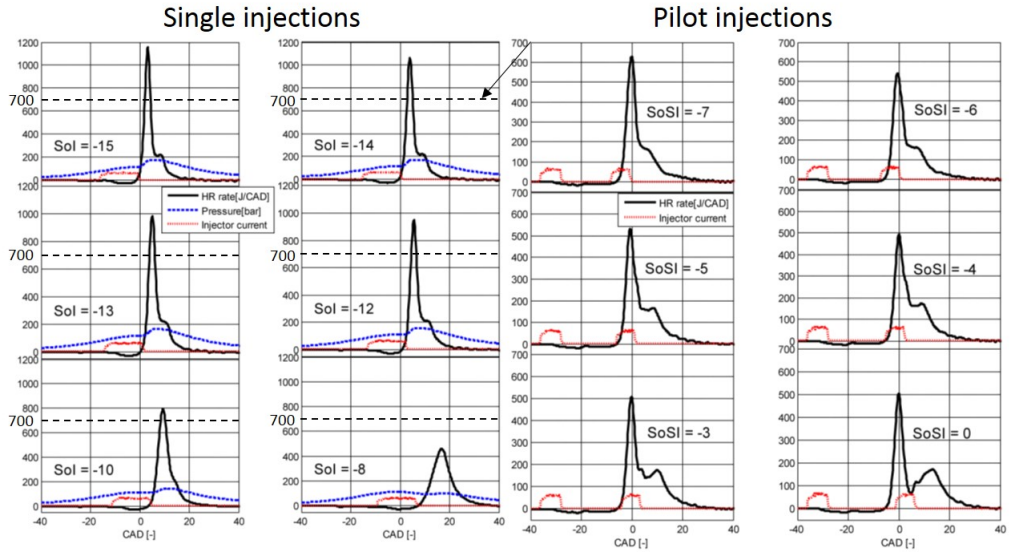


Figure 4.12: Comparison of heat release rates of single and pilot injection strategies

Figure 4.12 shows the heat release rates for single injection strategies as well as the effect of pilot injection strategies. As seen in the single injection cases, the highly volatile fuel quickly mixes with the ambient oxygen, and due to the high octane number of 107 RON the ignition delay gives rise to a high and short heat release and, consequently, a high pressure rise rate. These conditions limit the operating range, in this case between SOI of -14 to -10 CAD aTDC. -14 is the high pressure rise rate limit, and the retarded limit of -10 is due to combustion instability.

Double injection strategies with a pilot injection can be used to overcome these issues. The right columns in Figure 4.12 shows the heat release cases for those strategies. In these cases, the pilot injection is fixed at SOI -35 CAD aTDC, and the second injection is swept. An earlier injection would lead to combustion instability [75] and higher UHC and CO emissions, as seen in Figure 4.13. The emissions will be discussed later in this section.

All cases show a lower heat release peak than the single injection cases when applying a pilot injection. This is because the pilot injection duration signal is 52% of the total signal, and the pilot injection should thereby contain approximately half the injected fuel mass. The premixed heat release is then heavily decreased. The pilot injection triggers the combustion process, whereas the main injection reacts in a more diffusion-like manner. This strategy allows the SOC to be controlled by the pilot injection and the CA₅₀ by the main injection.

The pilot injection strategy leads to penalties in UHC and CO emissions, as seen in Figure 4.13, and consequently in the efficiency. The top sub-figure in Figure 4.13 describes the effect of shifting the pilot injection (start of first injection - SOFI). The center sub-figure shows

the main injection (start of second injection - (SoSI)) and the bottom sub-figure displays the variation in fuel mass repartition between the pilot and main injections. The dashed vertical lines are the fixed settings during the sweeps of the other parameters in this figure. The SOI of the pilot injection is limited by geometry. For this reason, the earliest feasible

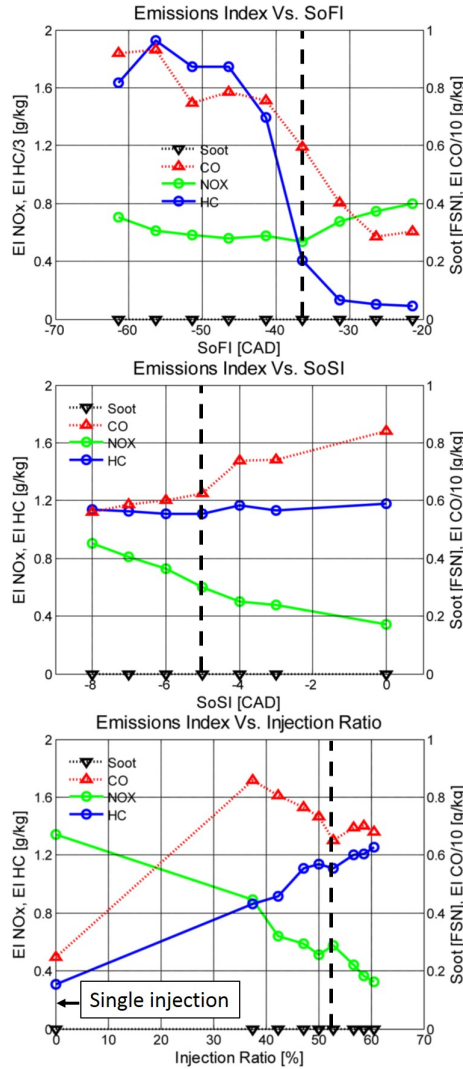


Figure 4.13: The top sub-figure describes the effect of shifting the pilot injection (SoFI). The center sub-figure shows the main injection (SoSI) and the bottom sub-figure displays the variation in fuel mass repartition between the pilot and main injections. The dashed vertical lines are the fixed settings during the sweeps of the other parameters in this figure.

injection is -35 CAD aTDC for the Scania geometry. The effect can be seen in both the HC and CO emissions as they decrease when the fuel begins to enter the piston bowl. A too early injection allows fuel to enter the squish region and consequently the ring pack crevice

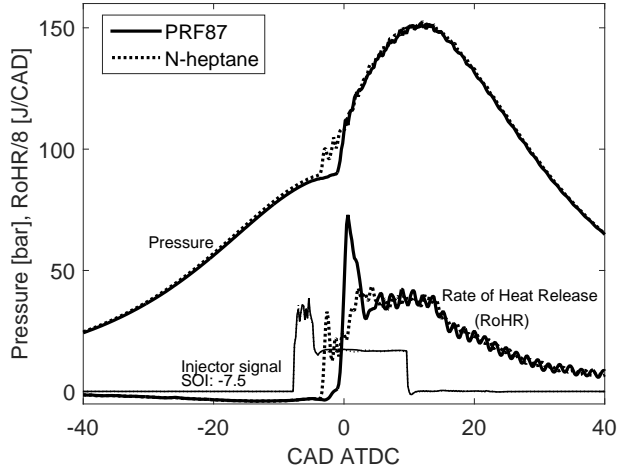


Figure 4.14: Comparison of the pressure traces and heat releases of gasoline and diesel.

volume. The sweep of the main injection shows low effect on the HC emissions, but CO increases and NO_x decrease. This could be caused by a decreased combustion efficiency and lower temperatures, aggravating the oxidation of CO. The bottom sub-figure in Figure 4.13, is shown to compare the emissions with the single injection case. Here the increase in UHC and CO emissions is clear when using pilot injections. This could partly be explained by fuel from the pilot injection escaping the piston bowl into crevices, forming over-lean zones.

Pilot injections decrease the premixed heat release and facilitate diffusion combustion of the fuel in the main injection. This allows higher loads while keeping the pressure rise rate at acceptable levels. In this case, higher loads could be achieved by increasing the duration of the main injection. In the next section, high load diffusion combustion is investigated in a comparison of fuels with low and high octane numbers.

4.2 Diffusion combustion

In Paper IV, high load diffusion combustion is applied in a comparison of gasoline and diesel, using PRF87 and *n*-heptane substitute reference fuels. Earlier work from [13, 78, 55] has shown the benefits of using gasoline, with lower soot emissions and higher efficiency. The first section will present a comparison between the pressure traces and heat releases of the two fuels, in a first step to evaluate factors that can reduce soot emissions.

4.2.1 Gasoline versus diesel

This study investigates the diffusion combustion under high load operation at 22 bar IMEP_g, in a comparison between diesel and gasoline fuels. For practical reasons pure *n*-heptane was used as a substitute for diesel, and a mixture of 87 percent iso-octane and 13 percent *n*-heptane by volume (PRF87) was used to resemble US pump gasoline. Specifications of the fuels can be found in section 2.4.

Figure 4.14 shows a comparison of the pressure and heat release traces from the combustion with the two respective fuels. All parameters are identical for the cases the cases, and only the fuel is changed.

The *n*-heptane behaves like a traditional diesel combustion case with a small premixed part, followed by a higher spray driven heat release, which is explained in detail in section 2.2. PRF87, has a higher resistance to auto-ignition and shows a longer ignition delay. This results in more mixing between fuel and air and a higher heat release peak at auto-ignition. The same is true for the pressure trace, since the longer premixing increases the pressure rise rate. As the spray driven part commences, the respective heat release and pressure traces merge for the two fuels. In previous work, correlations between the decay rate of the heat release has been shown to be strongly correlated to the late cycle soot oxidation rate and the engine out emissions [79, 80]. Since the decay rates in this experiment are closely coupled, it's thereby safe to assume that the oxidation rate is equal for the two fuels.

Focus is then shifted to the initial part of the combustion process. To influence the LoL and ignition delay, injection pressure and inlet temperature are varied. The two parameters are swept in three steps, generating a matrix of nine test points for respective fuel. Load and CA₅₀ is kept constant in the comparison, thus the injection duration and SOI are tuned for the nine different set-points. Like the results presented in Figure 4.14, no variation in parameters between the respective fuel are made.

Figure 4.15 include the heat release cases of *n*-heptane and PRF87. The curves show the influence by the inlet temperature and the fuel injection pressure sweeps. Blue lines correspond to a inlet temperature of 70°C, black to 90°C and the red to 110°C. The dashed line represents 1500 bar injection pressure, the solid 2000 bar and the dotted line 2300 bar. Markers are put on the premixed heat release peaks to simplify the comparison. The color corresponds to inlet temperature and the shape to the injection pressure.

Due to the higher resistance to autoignition the PRF87 cases show a longer ignition delay and a larger premixed part of the combustion. This means that more time is given for premixing, resulting in lower soot compared to *n*-heptane.

Decreasing the inlet temperature leads to a longer ignition delay for any given injection pressure, as seen in Figure 4.15. For the more premixed cases, a larger portion of the heat

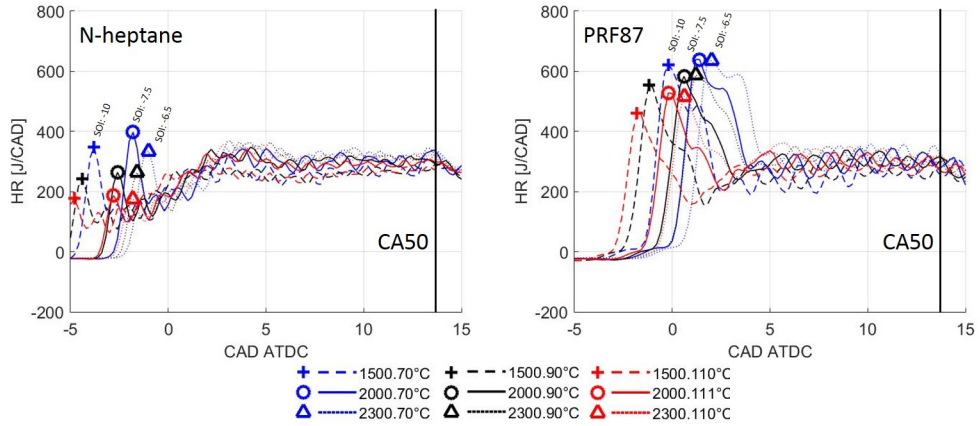


Figure 4.15: Rate of heat release of *n*-heptane and PRF87 as a function of CAD

release occurs in the premixed part, hence less fuel is burnt in the spray driven part. Having less spray driven combustion is also expected to decrease heat losses to the piston.

The longest ignition delay is given by an injection pressure of 1500 bar and 70°C. When increasing the injection pressure, the fuel mass injected per unit time increases and the mixing rate increases. For this reason the SOI has to be retarded to keep CA₅₀ constant. During the spray driven part of the heat release, the higher injection pressures show a slightly higher heat release, but the curves merge as CA₅₀ is reached.

Longer ignition delays lower the soot formation through increased premixing, and soot formation is also decreased with a longer LoL for the same reason [20]. The following section presents the results of the LoL measurement carried out these cases.

4.2.1.1 Lift off length

Through experiment in a combustion vessel, the quasi steady LoL is stated to correlate with ignition quality of the fuel, meaning that a higher octane number leads to a longer stabilized LoL [81]. For this reason, the air entrainment increases and less soot is produced, in a combustion engine. As mentioned in the parent section, the high octane fuels lower soot emission at higher loads compared to the low octane fuels. This leads to the question if different RON leads to different quasi-steady LoL.

The test matrix earlier described was used to investigate this question. First to test the autoignition quality, the PRF87 was compared with *n*-heptane. The conditions were varied with the ambient parameter of inlet temperature and injection pressure. The result from the LoL measurement is presented below.

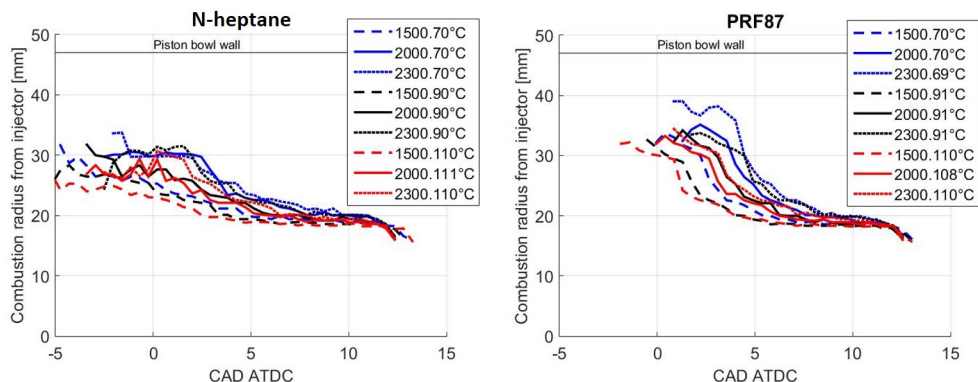


Figure 4.16: Lift-off lengths for different fuel injections pressures and inlet temperatures in a comparison of *n*-heptane and PRF87

The LoL of the two fuels are presented in Figure 4.16. The LoL is presented on the y-axis as a function of the CAD on the x-axis.

The PRF87 fuel, having higher resistance to auto ignition, travels further towards the bowl periphery before autoignition. In these cases the fuel even reaches the piston bowl wall before autoignition occurs. In most cases with PRF87 in Figure 4.16, the traces begin with a slight hump, meaning that the fuel that impinges the bowl wall and recirculate autoignite before a LoL is established. For this reason is the LoL first established at the peak of the hump. Figure 4.17 shows averaged HSV image at the start of combustion, both for *n*-heptane and PRF87. The distance to the piston bowl wall is here marked with a circle. For PRF87, combustion starts in the recirculated fuel after impinging the bowl wall, continues to travel along the wall and bowl floor, and seen "halos" around the point of impingement in Figure 4.17. As the sequence continues, the combustion region travels upstream the fuel until the impingement point is reached and a LoL is established. This phenomenon can also be seen in the heat release trace of PRF87 in Figure 4.15, as a hump after the main premixed heat release. This could be interpreted as a two step combustion, first with a premixed combustion in the recirculated fuel vapour and secondly in the premixed portion upstream of the fuel jet. This is merely based on observations and needs to be further investigated. If this is the case, the thermal properties of the quartz piston could play a role. The LoL established in the second step travels upstream the fuel jet towards the injector. While the combustion continues, the LoL rapidly decreases. A reason for this can be that the LoL of PRF87 directly interacts with the hot recirculated gases after impinging the bowl wall, hence a larger amount of the local hot gases are entrained in the fuel jet at the lift off position. The transient phase is hence quickly accelerated towards a stabilized position at the same level as *n*-heptane.

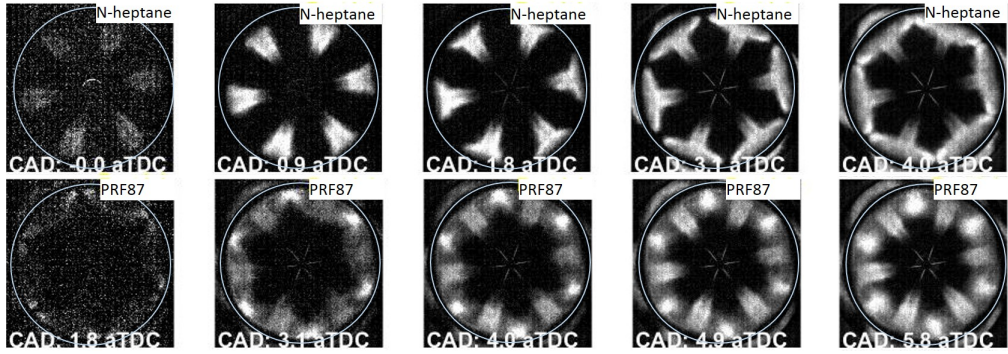


Figure 4.17: Averaged HSV images of *n*-heptane and PRF87 during the initial part of combustion.

n-heptane autoignites upstream in the fuel jet, before it impinges on the bowl wall. Thereby, the established LoL is closer to the final lift-off and less influenced by the hot gases of the recirculated combustion.

The LoLs converge for all the tested cases as they reach quasi steady conditions close to 8 CAD aTDC. All cases, no matter what fuel, merge into a common lift off just below 20 mm. Neither the injection pressure, ignition delay, nor inlet temperature affect the stabilized LoL. This implicates that it is the ambient conditions in the combustion chamber that has the major impact on the LoL. Studies of autoignition shows that for the ignition delay of PRF coincides as higher temperatures are reached, as seen in Figure 2.8.

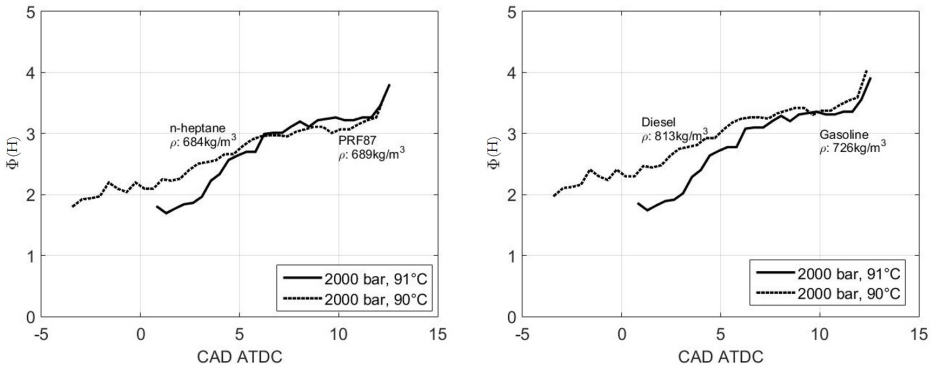


Figure 4.18: Equivalence ratio $\Phi(H)$ of *n*-heptane and PRF87 as a function of CAD aTDC.

These experiments were done with *n*-heptane and PRF87 which have similar density, 684 kg/m³ and 689 kg/m³ respectively, hence the fluid properties are the same. If using pump gasoline or diesel, with 813 kg/m³ and 726 kg/m³ respectively, the difference in LoL would probably be larger. Calculations of the local equivalence ratio at LoL ($\Phi(H)$) were per-

formed to investigate the effect of the difference in density, using Equation 2.2. The results are shown in Figure 4.18, showing the baseline case from each fuel, i.e. 2000 bar injection pressure and 90°C inlet temperature. The input LoL to the calculation is the same for the comparison, therefore only the effect of fuel density is shown on the $\Phi(H)$.

In line with the previous results, $\Phi(H)$ merges into a common value for all the fuel densities. The trend remains the same as the densities of the fuels are increased to the pump fuel standard, however at richer conditions with a $\Phi(H)$ closer to 3.5 for the quasi steady region at 8 CAD aTDC. The initial stages of the combustion show a larger separation in $\Phi(H)$, which implies that gasoline produces less soot, at least initially. Gasoline is a highly volatile fuel, which promote the evaporation, and allows the liquid length to decrease, and increase the fuel and air mixing [55].

This study show that all LoL converge into the same quasi steady position, no matter the octane number. This conclude that soot reduction cannot be explained with a higher octane number causing a longer quasi steady LoL. It also shows that the ambient parameters have no influence on the LoL, which means that the hot in cylinder bulk gases dominates the LoL.

Chapter 5

Summary

This chapter briefly summarizes the work resulting in this thesis.

Using a high octane fuel in compression ignition has been shown to facilitate low engine out soot and NO_x emissions while achieving high efficiency. Such fuels require different approaches to achieve stable combustion in different parts of the load range. This thesis goes through these load steps, from low to medium load using LTC (HCCI and PPC), to high load operation using diffusion combustion. Figure 5.1 shows a summary of the typical appearances of each combustion mode.



Figure 5.1: Summary of the different combustion modes used in this thesis

HCCI, which is described to the far left in Figure 5.1, is well known to achieve low engine out soot and NO_x , but suffers from UHC emissions due to fuel trapped in crevices not burning completely. The combustion stability is also known to be an issue due to the long ignition delay. The combustion sensitivity to the combustion chamber bulk temperature was analysed here.

The same sensitivity analysis was performed during a transition from HCCI to PPC. During this sweep, the level of premixing decreased, as seen when moving from the HCCI image to the left to the PPC image in the middle of Figure 5.1. Optical diagnostics show how the temperature dependence decreases as uniform combustion areas are formed. PPC,

like HCCI, suffers from UHC emissions. Post injection strategies were used in an attempt to reduce these emissions. Close-coupled post injections showed reductions in the UHC emissions, and optical diagnostics showed that the combustion areas associated with the post injection reach further into the combustion chamber. Fuel tracer PLIF was performed on the case to gain further insight, showing how fuel in the post injection reaches higher velocities in the wake of the first injection.

The intermediate stage between PPC and diffusion combustion is shown in the fourth image from the left of Figure 5.1. At an intermediate load a large premixed combustion is followed by a diffusion like combustion. Due to the combination of the higher load and the high degree of premixing, this intermediate load step suffers from high pressure rise rates. This was shown to be suppressed with double injection strategies. By distributing the fuel injections with one premixed charge and one diffusion like part, the initial premixed part decreases, which lowers the pressure rise rate.

Diffusion combustion at high load operation is shown to the far left image in Figure 5.1. The topic of this investigation aimed to address the underlying factors explaining the low engine out soot when using gasoline. It was initially hypothesised that higher octane fuels would have a longer LoL, thereby allowing more air entrainment and lower soot formation. A comparison between diesel and gasoline was performed. In contrast with the hypothesis, the investigation showed that the quasi steady LoL is the same for all cases, no matter what fuel or initial condition that are set. Two things are therefore implied. Firstly, the LoL is mainly dependent on the ambient conditions during combustion. As the jets experience elevated ambient temperatures due to hot combustion products, the fuel properties become less important. Secondly that there are other factors that contribute to the soot reduction with gasoline, like the ignition delay.

5.1 Thesis contributions

From a general point of view, this work contributes with a baseline of optical diagnostics of gasoline compression ignition in a quiescent combustion system, addressing possibilities and challenges with the concept. The main contributions are listed below:

- The full load range of gasoline compression ignition as been demonstrated in an optical engine, from HCCI, via the combustion mode of PPC, to diffusion combustion.
- The first description of gasoline combustion at high load operation in an optical engine is given.

- In this engine, the quasi steady LoL is dominated by the ambient conditions during combustion and shows no effect of octane number nor initial conditions.
- A continued insight in the mechanism behind UHC reduction with the utilization of close couple post injection is presented, where the results from the fuel PLIF measurements suggest that the post injection reach higher velocity in the wake of the main injection, thereby enriching over-lean zones in the recirculation zones of the combustion chamber.
- A method to analyse the combustion sensitivity to bulk temperature was found. Briefly summarized, it is based on running the engine in skip-fire mode during two or more consecutive combustion cycles, where the first cycle retrieves a fresh set of gases and the second cycle contains residual gases and higher bulk temperature from the first cycle.
- Design and demonstration of a new optical engine facilitating high load operation, that will contribute variety of future investigations.

Chapter 6

Bibliography

- [1] C Lyle Cummins. *Internal fire*. Carnot Press, 1976.
- [2] John Heywood. *Internal combustion engine fundamentals*. McGraw-Hill Education, 1988.
- [3] DieselNet emission standards. <https://www.dieselnets.com/standards/>. Accessed: 2017-04-04.
- [4] NASA global climate change. <https://climate.nasa.gov/causes/>. Accessed: 2017-04-04.
- [5] Daniel A Lashof and Dilip R Ahuja. Relative contributions of greenhouse gas emissions to global warming. *Nature*, 344(6266):529–531, 1990.
- [6] INTERNATIONAL ENERGY AGENCY. *World Energy Balances 2016*. OECD, 2016.
- [7] The Outlook for Energy: A View to 2040. *Exxon Mobil Corporation*, 2016.
- [8] Steven Chu and Arun Majumdar. Opportunities and challenges for a sustainable energy future. *nature*, 488(7411):294–303, 2012.
- [9] Berker Bilgin, Pierre Magne, Pawel Malysz, Yinye Yang, Vera Pantelic, Matthias Preindl, Alexandre Korobkine, Weisheng Jiang, Mark Lawford, and Ali Emadi. Making the Case for Electrified Transportation. *IEEE Transactions on Transportation Electrification*, 1(1):4–17, 2015.
- [10] Steven G Chalk and James F Miller. Key challenges and recent progress in batteries, fuel cells, and hydrogen storage for clean energy systems. *Journal of Power Sources*, 159(1):73–80, 2006.

- [11] Håkan Sundelin, Martin G H Gustavsson, and Stefan Tongur. The maturity of electric road systems. In *Electrical Systems for Aircraft, Railway, Ship Propulsion and Road Vehicles & International Transportation Electrification Conference (ESARS-ITEC), International Conference on*, pages 1–5. IEEE, 2016.
- [12] Bengt Johansson. *Förbränningsmotorer*. Division of Combustion Engines, LTH, 2006.
- [13] Gautam T Kalghatgi, Per Risberg, and Hans-Erik Ångström. Partially pre-mixed auto-ignition of gasoline to attain low smoke and low NO_x at high load in a compression ignition engine and comparison with a diesel fuel. SAE Technical Paper 2007-01-0006, 2007.
- [14] Irvin Glassman, Richard A Yetter, and Nick G Glumac. *Combustion*. Academic press, 2014.
- [15] Ulf Aronsson. *Processes in Optical Diesel Engines-Emissions Formation and Heat Release*. PhD thesis, 2011.
- [16] John E Dec. A conceptual model of DI diesel combustion based on laser-sheet imaging. SAE Technical Paper 970873, 1997.
- [17] Jeffrey D Naber and Dennis L Siebers. Effects of gas density and vaporization on penetration and dispersion of diesel sprays. SAE Technical Paper 960034, 1996.
- [18] Dennis L Siebers and Brian Higgins. Flame lift-off on direct-injection diesel sprays under quiescent conditions. SAE Technical Paper 2001-01-0530, 2001.
- [19] Guillaume Lequien, Zheming Li, Oivind Andersson, and Mattias Richter. Lift-Off Length in an Optical Heavy-Duty Diesel Engine: Effects of Swirl and Jet-Jet Interactions. *SAE International Journal of Engines*, 8(2015-24-2442):2188–2198, 2015.
- [20] Lyle M Pickett and Dennis L Siebers. Soot in diesel fuel jets: effects of ambient temperature, ambient density, and injection pressure. *Combustion and Flame*, 138(1):114–135, 2004.
- [21] Takeyuki Kamimoto and Myurng-hoan Bae. High combustion temperature for the reduction of particulate in diesel engines. Technical report, 1988.
- [22] Sanghoon Kook, Choongsik Bae, Paul C Miles, Dae Choi, and Lyle M Pickett. The influence of charge dilution and injection timing on low-temperature diesel combustion and emissions. SAE Technical Paper 2005-01-3837, 2005.
- [23] Lyle M Pickett and Dennis L Siebers. Non-sooting, low flame temperature mixing-controlled DI diesel combustion. SAE Technical Paper 2004-01-1399, 2004.

- [24] Christopher J Polonowski, Charles J Mueller, Christopher R Gehrke, Tim Bazyn, Glen C Martin, and Peter M Lillo. An experimental investigation of low-soot and soot-free combustion strategies in a heavy-duty, single-cylinder, direct-injection, optical diesel engine. *SAE International Journal of Fuels and Lubricants*, 5(2011-01-1812):51–77, 2011.
- [25] Ryan K Gehmlich, Cosmin E Dumitrescu, Yefu Wang, and Charles J Mueller. Leaner Lifted-Flame Combustion Enabled by the Use of an Oxygenated Fuel in an Optical CI Engine. *SAE International Journal of Engines*, 9(2016-01-0730):1526–1543, 2016.
- [26] John E Dec. Advanced compression-ignition engines - Understanding the in-cylinder processes. *Proceedings of the Combustion Institute*, 32 II(2):2727–2742, 2009.
- [27] Adam B Dempsey, Scott J Curran, and Robert M Wagner. A perspective on the range of gasoline compression ignition combustion strategies for high engine efficiency and low NO_x and soot emissions: Effects of in-cylinder fuel stratification. *International Journal of Engine Research*, 17(8):897–917, 2016.
- [28] Allen W Bill Gray and Thomas W Ryan. Homogeneous charge compression ignition (HCCI) of diesel fuel. SAE Technical Paper 971676, 1997.
- [29] Magnus Christensen, Bengt Johansson, and Patrik Einewall. Homogeneous charge compression ignition (HCCI) using isooctane, ethanol and natural gas-a comparison with spark ignition operation. SAE Technical Paper 972874, 1997.
- [30] Rudolf H Stanglmaier and Charles E Roberts. Homogeneous charge compression ignition (HCCI): benefits, compromises, and future engine applications. SAE Technical Paper 1999-01-3682, 1999.
- [31] Shigeru Onishi, Souk Hong Jo, Katsuji Shoda, Pan Do Jo, and Satoshi Kato. Active thermo-atmosphere combustion (ATAC)-a new combustion process for internal combustion engines. SAE Technical Paper 790501, 1979.
- [32] Robert H Thring. Homogeneous-charge compression-ignition (HCCI) engines. Technical report, 1989.
- [33] Magnus Christensen and Bengt Johansson. Influence of mixture quality on homogeneous charge compression ignition. *SAE transactions*, 107(724):948–960, 1998.
- [34] John E Dec, Wontae Hwang, and Magnus Sjöberg. An investigation of thermal stratification in HCCI engines using chemiluminescence imaging. SAE Technical Paper 2006-01-1518, 2006.
- [35] Hans Seyfried, Jimmy Olofsson, Johan Sjöholm, Mattias Richter, Marcus Aldén, Andreas Vressner, Anders Hultqvist, and Bengt Johansson. High-speed PLIF imaging for

- investigation of turbulence effects on heat release rates in HCCI combustion. SAE Technical Paper 2007-01-0213, 2007.
- [36] Yoshinaka Takeda, Nakagome Keiichi, and Niimura Keiichi. Emission characteristics of premixed lean diesel combustion with extremely early staged fuel injection. SAE Technical Paper 961163, 1996.
 - [37] Sage Kokjohn, Rolf D Reitz, Derek Splitter, and Mark Musculus. Investigation of fuel reactivity stratification for controlling PCI heat-release rates using high-speed chemiluminescence imaging and fuel tracer fluorescence. *SAE International Journal of Engines*, 5(2012-01-0375):248–269, 2012.
 - [38] Håkan Persson, Bengt Johansson, and Alfredo Remón. The effect of swirl on spark assisted compression ignition (SACI). SAE Technical Paper 2007-01-1856, 2007.
 - [39] Shuji Kimura, Osamu Aoki, Hiroshi Ogawa, Shigeo Muranaka, and Yoshiteru Enomoto. New combustion concept for ultra-clean and high-efficiency small DI diesel engines. SAE Technical Paper 1999-01-3681, 1999.
 - [40] Shuji Kimura, Osamu Aoki, Yasuhisa Kitahara, and Eiji Aiyoshizawa. Ultra-clean combustion technology combining a low-temperature and premixed combustion concept for meeting future emission standards. SAE Technical Paper 2001-01-0200, 2001.
 - [41] Paul C Miles, Dae Choi, Lyle M Pickett, I P Singh, Naeim Henein, Bret RempelEwert, H Yun, and Rolf D Reitz. Rate-limiting processes in late-injection, low-temperature diesel combustion regimes. In *Proc. THIESEL 2004 Conference*, pages 429–447, 2004.
 - [42] Vittorio Manente, Claes-Goeran Zander, Bengt Johansson, Per Tunestal, and William Cannella. An advanced internal combustion engine concept for low emissions and high efficiency from idle to max load using gasoline partially premixed combustion. SAE Technical Paper 2010-01-2198, 2010.
 - [43] Martin Tuner, Bengt Johansson, Philip Keller, and Michael Becker. Loss analysis of a HD-PPC engine with two-stage turbocharging operating in the European stationary cycle. SAE Technical Paper 2013-01-2700, 2013.
 - [44] Helgi Fridriksson, Bengt Sundén, Martin Tunér, and Öivind Andersson. Heat Transfer in Diesel and Partially Premixed Combustion engines; A Computational Fluid Dynamics Study. *Heat Transfer Engineering*, (just-accepted), 2016.
 - [45] Kazuhiro Akihama, Yoshiki Takatori, Kazuhisa Inagaki, Shizuo Sasaki, and Anthony M Dean. Mechanism of the smokeless rich diesel combustion by reducing temperature. SAE technical paper 2001-01-0655, 2001.

- [46] Mark P B Musculus, Paul C Miles, and Lyle M Pickett. Conceptual models for partially premixed low-temperature diesel combustion. *Progress in Energy and Combustion Science*, 39(2):246–283, 2013.
- [47] Duksang Kim, Isaac Ekoto, William F Colban, and Paul C Miles. In-cylinder CO and UHC imaging in a light-duty diesel engine during PPCI low-temperature combustion. *SAE International Journal of Fuels and Lubricants*, 1(2008-01-1602):933–956, 2008.
- [48] Mark P. B. Musculus, Thierry Lachaux, Lyle M. Pickett, and Cherian A. Idicheria. End-of-Injection Over-Mixing and Unburned Hydrocarbon Emissions in Low-Temperature- Combustion Diesel Engines. *Sae*, 2007-01-09(724):776–0790, 2007.
- [49] Sylvain Mendez, Julian T Kashdan, Gilles Bruneaux, Benoist Thirouard, and Franck Vangraefschep. Formation of unburned hydrocarbons in low temperature diesel combustion. *SAE International Journal of Engines*, 2(2009-01-2729):205–225, 2009.
- [50] Mark P B Musculus and Kyle Kattke. Entrainment waves in diesel jets. *SAE International Journal of Engines*, 2(2009-01-1355):1170–1193, 2009.
- [51] Clément Chartier, Oivind Andersson, Bengt Johansson, Mark Musculus, and Mohan Bobba. Effects of post-injection strategies on near-injector over-lean mixtures and unburned hydrocarbon emission in a heavy-duty optical diesel engine. *SAE International Journal of Engines*, 4(2011-01-1383):1978–1992, 2011.
- [52] Jacqueline O’Connor, Mark P B Musculus, and Lyle M. Pickett. Effect of post injections on mixture preparation and unburned hydrocarbon emissions in a heavy-duty diesel engine. *Combustion and Flame*, 170:111–123, 2016.
- [53] Vittorio Manente, Bengt Johansson, and Per Tunestal. Partially premixed combustion at high load using gasoline and ethanol, a comparison with diesel. SAE Technical Paper 2009-01-0944, 2009.
- [54] Reed Hanson, Derek Splitter, and Rolf D Reitz. Operating a heavy-duty direct-injection compression-ignition engine with gasoline for low emissions. SAE Technical Paper 2009-01-1442, 2009.
- [55] Liang Zheng, Xiao Ma, Zhi Wang, and Jianxin Wang. An optical study on liquid-phase penetration, flame lift-off location and soot volume fraction distribution of gasoline–diesel blends in a constant volume vessel. *Fuel*, 139:365–373, 2015.
- [56] Sanghoon Kook and Lyle M Pickett. Effect of fuel volatility and ignition quality on combustion and soot formation at fixed premixing conditions. *SAE International Journal of Engines*, 2(2009-01-2643):11–23, 2009.

- [57] Leif Hildingsson, Gautam Kalghatgi, Nigel Tait, Bengt Johansson, and Andrew Harrison. Fuel octane effects in the partially premixed combustion regime in compression ignition engines. *SAE Technical Paper 2009-01-2648*, 2009.
- [58] K Fieweger, Ro Blumenthal, and G Adomeit. Self-ignition of SI engine model fuels: a shock tube investigation at high pressure. *Combustion and Flame*, 109(4):599–619, 1997.
- [59] Dan DelVescovo, Sage Kokjohn, and Rolf Reitz. The development of an ignition delay correlation for PRF fuel blends from PRFo (n-heptane) to PRF100 (iso-octane). *SAE International Journal of Engines*, 9(2016-01-0551):520–535, 2016.
- [60] Shigeyuki Tanaka, Ferran Ayala, James C Keck, and John B Heywood. Two-stage ignition in HCCI combustion and HCCI control by fuels and additives. *Combustion and flame*, 132(1):219–239, 2003.
- [61] Raul Payri, Antonio García, Vicent Domenech, Russell Durrett, and Alejandro H Plazas. An experimental study of gasoline effects on injection rate, momentum flux and spray characteristics using a common rail diesel injection system. *Fuel*, 97:390–399, 2012.
- [62] Uwe Horn, Helena Persson, Rolf Egnell, Oivind Andersson, and Erik Rijk. The Influence of Fuel Properties on Transient Liquid-Phase Spray Geometry and on CI-Combustion Characteristics. *SAE International Journal of Engines*, 2(2009-01-2774):300–311, 2009.
- [63] Paul C Miles. The history and evolution of optically accessible research engines and their impact on our understanding of engine combustion. In *ASME 2014 internal combustion engine division fall technical conference*, pages V002To8A003–V002To8A003. American Society of Mechanical Engineers, 2014.
- [64] Lloyd Withrow and T A Boyd. Photographic flame studies in the gasoline engine. *Industrial & Engineering Chemistry*, 23(5):539–547, 1931.
- [65] Fred W Bowditch. A new tool for combustion research a quartz piston engine. *SAE Technical Paper 610002*, 1961.
- [66] Dennis L Siebers. Liquid-phase fuel penetration in diesel sprays. *SAE technical paper 980809*, 1998.
- [67] Liang Zheng, Yunliang Qi, Xu He, and Zhi Wang. Visualization of partially premixed combustion of gasoline-like fuel using high speed imaging in a constant volume vessel. *SAE International Journal of Engines*, 5(2012-01-1236):1320–1329, 2012.

- [68] Christoph Espey and John E Dec. Diesel engine combustion studies in a newly designed optical-access engine using high-speed visualization and 2-D laser imaging. SAE Technical Paper 930971, 1993.
- [69] Ulf Aronsson, Hadeel Solaka, Clément Chartier, Oivind Andersson, and Bengt Johansson. Impact of mechanical deformation due to pressure, mass, and thermal forces on the in-cylinder volume trace in optical engines of Bowditch design. SAE Technical Paper 2011-26-0082, 2011.
- [70] Ulf Aronsson, Hadeel Solaka, Guillaume Lequien, Oivind Andersson, and Bengt Johansson. Analysis of errors in heat release calculations due to distortion of the in-cylinder volume trace from mechanical deformation in optical diesel engines. *SAE International Journal of Engines*, 5(2012-01-1604):1561–1570, 2012.
- [71] Takayuki Fuyuto, Takafumi Matsumoto, Yoshiaki Hattori, Ko Kugimoto, Taketoshi Fujikawa, Kazuhiro Akihama, and Hisaki Ito. A New Generation of Optically Accessible Single-Cylinder Engines for High-Speed and High-Load Combustion Analysis. *SAE International Journal of Fuels and Lubricants*, 5(2011-01-2050):307–315, 2011.
- [72] Ulf Aronsson, Clement Chartier, Uwe Horn, Öivind Andersson, Bengt Johansson, and Rolf Egnell. Heat release comparison between optical and all-metal hsd diesel engines. SAE Technical Paper 2008-01-1062, 2008.
- [73] Joakim Rosell. *Optical Diagnostic Techniques Applied in Practical Combustion Devices and Processes*. PhD thesis, 2016.
- [74] Zhenkan Wang, Sara Lonn, Alexios Matamis, Oivind Andersson, Martin Tuner, Marcus Alden, and Mattias Richter. Transition from HCCI to PPC: Investigation of Fuel Distribution by Planar Laser Induced Fluorescence (PLIF). *SAE International Journal of Engines*, 10(2017-01-0748), 2017.
- [75] Sara Lonn, Alexios Matamis, Martin Tuner, Mattias Richter, and Oivind Andersson. Optical Study of Fuel Spray Penetration and Initial Combustion Location under PPC Conditions. SAE Technical Paper 2017-01-0752, 2017.
- [76] Hultqvist Anders, Magnus Christensen, Bengt Johansson, Axel Franke, Mattias Richter, and Marcus Aldén. A study of the homogeneous charge compression ignition combustion process by chemiluminescence imaging. SAE Technical Paper, 1999.
- [77] Öivind Andersson, Joop Somhorst, Ronny Lindgren, Roger Blom, and Mattias Ljungqvist. Development of the Euro 5 combustion system for volvo cars’ 2.4. I diesel engine. SAE Technical Paper 2009-01-1450, 2009.

- [78] Mengqin Shen, Martin Tuner, Bengt Johansson, and William Cannella. Effects of EGR and intake pressure on PPC of conventional diesel, gasoline and ethanol in a heavy duty diesel engine. SAE Technical Paper, 2013.
- [79] Ulf Aronsson, Clément Chartier, Öivind Andersson, Rolf Egnell, Johan Sjöholm, Mattias Richter, and Marcus Aldén. Analysis of the correlation between engine-out particulates and local ϕ in the lift-off region of a heavy duty diesel engine using raman spectroscopy. *SAE International Journal of Fuels and Lubricants*, 2(2009-01-1357):645–660, 2009.
- [80] Guillaume Lequien, Öivind Andersson, Per Tunestal, and Magnus Lewander. A correlation analysis of the roles of soot formation and oxidation in a heavy-duty diesel engine. SAE Technical Paper 2013-01-2535, 2013.
- [81] Lyle M Pickett, Dennis L Siebers, and Cherian A Idicheria. Relationship between ignition processes and the lift-off length of diesel fuel jets. SAE Technical Paper 2005-01-3843, 2005.

Chapter 7

Summary of papers

7.1 Paper I

Gasoline PPC: A Parametric Study of Late Cycle Mixing Conditions using a Predictive Two-zone SRM Modeling Tool

Marcus Lundgren¹, Martin Tunér¹, Bengt Johansson¹, Simon Bjerkborn², Karin Frojd², Arne Andersson³, Bincheng Jiang³, Fabian Mauss⁴

¹*Division of Combustion Engines, Lund University, Sweden*

²*LOGE AB*

³*Volvo AB*

⁴*BTU Cottbus*

SAE Technical Paper 2013-01-2621

This paper deals with the effect of the in-cylinder turbulence intensity on the combustion, using a zero dimensional stochastic reactor model (SRM). In-cylinder turbulence origin from several factors, such as, intake flow, injection pressure and timing, and piston shape. Analyses aim to investigate variations in turbulence parameters and the affect on air and fuel distribution, prior and during the combustion process. Results from the investigation show that the two-zone SRM is suitable for prediction of the PPC conditions and is able to run simulations at an average of 25 min/cycle. The findings of the parametric study showed, that a higher mixing intensity is preferable to longer mixing duration before the start of combustion as it decreases pressure rise rate without penalizing combustion efficiency.

This work was performed in collaboration with Volvo AB and Loge. I put together the experimental matrix, using design of experiment. This was implemented with Matlab in connection with the simulation software. Thereby a large number of simulations was done continuously.

The results was post processed by me. The paper was written together with Martin Tunér.

7.2 Paper II

Optical Study on Combustion Transition from HCCI to PPC with Gasoline Compression Ignition in a HD Engine

Marcus Lundgren¹, Öivind Andersson¹, Bengt Johansson¹, Joakim Rosell², Mattias Richter², Marcus Aldén², Arne Andersson³

¹*Division of Combustion Engines, Lund University, Sweden*

²*Division of Combustion Physics, Lund University, Sweden*

³*Volvo AB*

SAE Technical Paper 2016-01-0768

This paper deals with the transition between HCCI to PPC. Results show that retarded injections show less cycle-to-cycle variation due to temperature variations. Advanced in-bowl injections show a stochastic behaviour in the location of the first combustion, due to large variations in local fuel rich zones. For the double injection case the main injection cools the bulk temperature and hence delays the start of combustion before igniting in the fuel rich zones.

This was the first performed experiments of the newly built optical engine. The experimental setup was design and mainly built by me and the technician Tomas Lindén. Experiments were performed together with Joakim Rosell. I designed the experimental matrix and post-processed the data from a combustion perspective and Joakim Rosell from a diagnostics perspective. The paper was written together with Joakim Rosell, Bengt Johansson and Öivind Andersson

7.3 Paper III

Effects of post-injections strategies on UHC and CO at gasoline PPC conditions in a Heavy-duty optical engine

Marcus Lundgren¹, Öivind Andersson¹, Martin Tunér¹, Zhenkan Wang², Alexios Matamis², Mattias Richter², Marcus Aldén², Arne Andersson³

¹*Division of Combustion Engines, Lund University, Sweden*

²*Division of Combustion Physics, Lund University, Sweden*

³*Volvo AB*

SAE Technical Paper 2017-01-0753

This paper deals with means to reduce UHC and CO in PPC using post injections. Typical

sources of these emissions are crevice, squish and near injector regions of the combustion chamber. This work deals with the latter. Results show reduction in both CO and UHC with close coupled injections. Additionally a large post injection show the largest reduction in UHC. Analysis show that injection that finish prior to combustion both increases the recirculation of fuel thus reaching further into the combustion chamber, and decrease visible dribble. These factors are hence decreasing the UHC in the area near the injector. General observations show that the partition of fuel between the injections have the largest impact on the CO while the dwell time affects UHC emissions. Injector dribble shows similar trends as with UHC, thus it's a significant contributor to the UHC emissions.

In this work I designed the experimental matrix. Experiments were performed together with Zhenkan Wang and Alexios Matamis. I post-processed the data and wrote the paper together with Öivind Andersson

7.4 Paper iv

Lift-off Lengths of Gasoline and Diesel at High Load Operation in a Optical Heavy-Duty Engine

Marcus Lundgren¹, Öivind Andersson¹, Pablo Garcia¹, Zhenkan Wang², Alexios Matamis², Mattias Richter², Marcus Aldén², Arne Andersson³

¹*Division of Combustion Engines, Lund University, Sweden*

²*Division of Combustion Physics, Lund University, Sweden*

³*Volvo AB*

To be submitted to Fuels Journal

This work compare gasoline and diesel at high load operation of 21 bar IMEPg. Earlier studies presented reduction in the engine out soot with gasoline. This is thought to be related with increased lift-off lengths with high octane fuels, in contrast to high cetane fuels such as diesel. Other studies suggest that the ambient conditions at a quiescent lift-off length is a strong factor in deciding the lift-off length. This work test these statement in the following experiment. Sweeps were made in injection pressure and inlet temperature, which are factors that affect the air entrainment in diffusion combustion. The result show that no matter the fuel nor initial conditions, the lifted flame reach equal an quasi steady lift-off lengths. This implies that the ambient conditions is the main driver to the lift-off length. Although, in the initial stages of combustion the ignition delay gasoline is longer, allow the fuel to reach further before igniting, thus the premixed part increases. Results show that the transition from the established, to the quasi steady lift-off length, is assumed to be caused by the entrainment of hot recirculated gases. Where as for diesel the transition is slower, since the autoignition occurs further upstream, longer from the recirculated hot gases.

I designed the experiment matrix for this work. The experiments were performed together with Zhenkan Wang and Alexios Matamis. I were in charge of operating the engine while my colleagues operated the diagnostics equipment. I post-processed the data and wrote the paper together with Öivind Andersson

7.5 Paper v

Sensitivity Analysis Study on Ethanol Partially Premixed Combustion

Mehrzad Kaiadi¹, Bengt Johansson¹, Marcus Lundgren¹, John Gaynor²

¹*Division of Combustion Engines, Lund University, Sweden*

²*Scania CV AB*

SAE International Journal of Engines, 2013-01-0269

The objective of this work was initially to investigate the required operating conditions for PPC with ethanol. A sensitivity analysis was performed to understand how parameters such as lambda, EGR rate, injection pressure and inlet temperature influence the combustion in terms of controllability, stability, emissions and thermodynamic efficiency. Investigations have been performed experimentally on a single cylinder heavy duty engine where each of the parameters swept one at time. The results showed that the combustion is not sensitive to changes in injection pressure but the adjustments in lambda, EGR and inlet temperature should be controlled very carefully as there are clear limitations for each of these parameters. These limitations are highlighted and presented in this study. Engine-out soot emissions showed to be detectable only once the global lambda is low in combination with high EGR rates.

The first author, Mehrzad Kaiadi, took the main responsibility in writing the paper. I assisted during the experiments with mechanical work and finding the baseline operating points which lead up the experimental matrix. I contributed in the data post processing and the paper writing.

7.6 Paper vi

Experimental Investigation on different Injection Strategies for Ethanol Partially Premixed Combustion

Mehrzad Kaiadi¹, Bengt Johansson¹, Marcus Lundgren¹, John Gaynor²

¹*Division of Combustion Engines, Lund University, Sweden*

²*Scania CV AB*

SAE Technical Paper 2013-01-0281

The objective of this research was to investigate a suitable injection strategy for PPC combustion with ethanol. Extensive experimental investigations were performed on a single-cylinder heavy-duty engine. The number of injections, injection timings and the ratio between the injection pulses was varied and the combustion behaviour was investigated at medium and low loads. The engine performance was evaluated in terms of controllability, stability, combustion noise, emissions and efficiencies. Additionally, a comparison between single and double-injection strategies was performed. The results indicated that the double injection strategy should be preferred for PPC fuelled with ethanol, since double injection strategy offers good combustion controllability and combustion performance (i.e. low emissions and high efficiency) while keeping the combustion noise at low levels.

The first author, Mehrzad Kaiadi, took the main responsibility in writing the paper. I assisted during the experiments with mechanical work and finding the baseline operating points which lead up the experimental matrix. I contributed in the data post processing and the paper writing.